Saudi Pharmaceutical Journal 30 (2022) 793–814

Contents lists available at ScienceDirect

Saudi Pharmaceutical Journal

journal homepage: www.sciencedirect.com

Original article

Phytochemical analysis and comprehensive evaluation of pharmacological potential of *Artemisia brevifolia* Wall. ex DC

Syeda Tayyaba Batool Kazmi [a,b], Iffat Naz [c,*], Syeda Saniya Zahra [a], Hamna Nasar [a], Humaira Fatima [a], Ayesha Shuja Farooq [d], Ihsan-ul Haq [a,*]

[a] Department of Pharmacy, Faculty of Biological Sciences, Quaid-i-Azam University, Islamabad 45320, Pakistan
[b] Department of Rehabilitation and Health Sciences, Iqra Univerity Islamabad Campus, Chak Shehzad, Islamabad 45320, Pakistan
[c] Department of Biology, Science Unit, Deanship of Educational Services, Qassim University, Buraidah 51452, Saudi Arabia
[d] Department of Biochemistry, Science Unit, Deanship of Educational Services, Qassim University, Buraidah 51452, Saudi Arabia

ARTICLE INFO

Article history:
Received 10 January 2022
Accepted 19 March 2022
Available online 29 March 2022

Keywords:
Antimicrobial
Artemisia
Cytotoxicity
Enzyme inhibition
Genotoxicity
HRMS

ABSTRACT

Multitude of diseases and side effects from conventional drugs have surged the use of herbal remedies. Thus, the current study aimed to appraise various pharmacological attributes of *Artemisia brevifolia* Wall. ex DC. Extracts prepared by successive solvent extraction were subjected to phytochemical and multimode antioxidant assays. Various polyphenolics and artemisinin derivatives were detected and quantified using RP-HPLC analysis. Compounds present in methanol (M) and distilled water (DW) extracts were identified using high resolution mass spectrometry (HRMS). Extracts were pharmacologically evaluated for their antibacterial, antifungal, antimalarial, antileishmanial and antidiabetic potentials. Moreover, cytotoxicity against *Artemiasalina,* human cancer cell lines and isolated lymphocytes was assessed. Genotoxicity was evaluated using comet, micronucleus and chromosomal aberration assays. Lastly, anti-inflammatory potential was determined through a series of *in vitro* and *in vivo* assays using BALB/c mice.

Maximum extract recovery (5.95% w/w) was obtained by DW extract. Highest phenolics and flavonoids content, total antioxidant capacity, total reduction potential, percentfree radical scavenging, β-carotene scavenging and iron chelating activities were exhibited by M extract. RP-HPLC analysis revealed significant amounts of various polyphenolic compounds (vanillic acid, syringic acid, emodin and luteolin), artemisinin, dihydro artemisinin, artesunate and artemether in ethyl acetate (EA) extract. Total 40 compounds were detected through HRMS. A noteworthy antimicrobial activity (MIC 22.22 μg/ml) was exhibited by EA extract against *A. fumigatus* and several bacterial strains. Maximum antimalarial, antileishmanial, brine shrimp lethality and cytotoxic potential against cancer cells was manifested by EA extract. None of the extracts exhibited genotoxicity and toxicity against isolated lymphocytes. Highest α-amylase and α-glucosidase inhibition capacities were demonstrated by DW extract. Various *in-vivo* anti-inflammatory models revealed significant ($p < 0.05$) anti-inflammatory potential of M and DW extracts. In conclusion, present findings divulged theremarkable pharmacological potential of *A. brevifolia* and endorse its richness in artemisinin.

Abbreviations: CL, Comet Length; DMEM, Dulbecco Modified Eagle's Medium; DPPH, 2,2-diphenyl-1-picrylhydrazyl; DMSO, Dimethyl sulfoxide; HEPES, N-2-hydroxyethylpiperazine–N-2-ethanesulfonic acid; HRMS, High Resolution Mass Spectroscopy; IC_{50}, 50% Inhibitory Concentration; LD_{50}, Lethal Dose Causing 50% Mortality; MIC, Minimum Inhibitory Concentration; MTT, 3-(4,5-dimethylthiazol-2-yl)-2,5-diphenyl tetrazolium bromide; MN, Micronucleus; NAMP, Number of Aberrant Metaphase; NDI, Nuclear Division Index; RP-HPLC, Reverse Phase-High Performance Liquid Chromatography; ZOI, Zone of Inhibition.

* Corresponding authors.
E-mail addresses: iffatkhattak@yahoo.com (I. Naz), Hfchughtai@qau.edu.pk (H. Fatima), a.muhammad@qu.edu.sa (A. Shuja Farooq), ihsn99@yahoo.com (I.-u. Haq).

Peer review under responsibility of King Saud University.

Production and hosting by Elsevier

https://doi.org/10.1016/j.jsps.2022.03.012
1319-0164/

1. Introduction

Plants are an integral part of life on earth. They form the basis of traditional medicinal system since ancient times. An incredibly growing tendency to use natural remedies has been witnessed both in developed and developing countries. This is quite evident from the fact that more than 40% of prescribed drugs in the world are mainly derived from herbal source. The process of natural product drug discovery involves multifaceted scientific approaches including ethnopharmacology and reverse pharmacology. These *trans*-disciplinary endeavors extend from gathering the folk knowledge of indigenous people to quasi drug development and provision of better and safer lead compounds (Shelar and Shirote, 2011). Legacy of traditional medicines established over hundreds of years by hit and trial on human subjects comprehend the valuable biomedical information, which can be uncovered through modern approaches. One such underexplored folklore is *Artemisia brevifolia* Wall. ex DC. (tarkha), from genus *Artemisia*, which is one of the largest and most widely distributed genera of the Asteraceae family. Several of its species are frequently utilized for the treatment of malaria, hepatitis, cancer, inflammation and microbial infections. Genus *Artemisia* (Worm wood, Mug word, Sagebrush or Tarragon) is rich in aromatic plants, which by virtue of the presence of monoterpenes and sesquiterpenes possess a characteristic scent or taste. These compounds also are responsible for their application in folk medicine (Koul et al., 2018).

A. brevifolia, a woody rooted herb, is the native plant of Northern India, Pakistan and Afghanistan. Growing widely in stony landscapes of Pakistan, *A. brevifolia* abounds in remote areas of Baltistan, Chitral, Gilgit, Swat, Khaghan, Deosai planes and Astor. The understudy species grows in stony topography with low humidity, sandy soils and usually covers the sun facing inclines of dry mountains. *A. brevifolia*is a 14–35 cm tall herb with a characteristic aromatic fragrance and whitish green color. Itsstems have a purplish shade. Flowering period of the plant is from August to September (Ashraf et al., 2010).

Traditionally, its decoction and powder are used as purgative and vermifuge. It is also employed to treat a number of ear, nose and throat related ailments as well as respiratory and gastric disorders by different native communities of Pakistan (Nadeem et al., 2013). Very limited scientific data is available regarding its pharmacological uses and only its anthelmintic use has been validated(Ashraf et al., 2010). *A. brevifolia,* though abundantly growing, is considered a troublesome weed and its dried stems are used as a source of fire(Hayat et al., 2009).

There is no evidence of systematic and organized bio-chemical screening of this species that could demonstrate the pharmacological potential of this ethnomedicinally important plant. Thus, the present study was planned to transform a bio-waste into a therapeutically active drug candidate by employing a battery of bioassays. Chemical and pharmacological profile of the plant was established by analyzing its extracts of escalating polarity for the presence of phytochemical compounds, antioxidant, antimicrobial, cytotoxic, antiprotozoal and enzyme inhibition potential. To the best of our knowledge, it is the first report highlighting pharmacological potential of *A. brevifolia*.

2. Material and methods

2.1. Chemicals and solvents

Solvents (n-Hexane, ethyl acetate, methanol, dimethyl sulfoxide (DMSO), trichloroacetic acid (TCA), lamda carrageenan, sea salt, napthylenediamine, croton oil, gallic acid, artemisinin, artesunate, artemether, dihydroadtemisinin, syringic acid, luteolin, tween 80, linoleic acid, gentisic acid, human serum and histopaque-1077 were bought from Sigma-Aldrich (Germany). Folin-Ciocalteu (FC) reagent, amphotericin B, clotrimazole, cefixime, roxithromycin and phosphate buffer (PB) were purchased from Riedel-de-Haen (Germany). Sabourad dextrose agar (SDA), α-glucosidase enzyme, α-Amylase enzyme, EDTA, RPMI-1640 culture media, Dulbecco's modified eagle medium (DMEM), sodium bicarbonate ($NaHCO_3$), normal melting point agarose (NMPA), low melting point agarose (LMPA) 3-(4,5-Dimethylthiazol-2-yl)-2,5-diphenyltetrazolium bromide (MTT) powder, N-2-hydroxyethylpiperazine–N-2-ethanesulfonic acid (HEPES), trisHCl, sodium carbonate (Na_2CO_3), starch, p-nitrophenyl-D-glucopyranose, sulphanilamide, phosphoric acid, acetonitrile, emodin, vanillic acid, β-carotene, ferulic acid, catechin, hydroethidine, trypsin, cytochalasin B, giemsa stain and colchicinewere bought from Merck, KGaA (Darmstadt, Germany). Acetic acid, triton X-100, ethidium bromide, dried instant yeast, heat inactivated fetal bovine serum (HIFBS) and acarbose were bought from Merck-Schuchardt (USA). Unless otherwise stated, all chemicals were procured from Sigma-Aldrich (USA).

2.2. Cell lines

Human cancer cell lines including leukemia cell line (THP-1, ATCC-TIB-202), hepatocellular carcinoma cell line (Hep G2, ATCC-HB-8065), ovarian cancer cell line (A2780, ATCC-CRL-2772), hormone responsive breast cancer cell line (MCF-7, ATCC-HTB-22), colorectal adenocarcinoma cell line (HT-29, ATCC-HTB-38) and prostate cancer cell line (DU-145, ATCC-HTB-81) were used in the study.

2.3. Microbial strains

Nine bacterial strains including *Klebsiella pneumoniae* (ATCC-1705), *Staphylococcus aureus* (ATCC- 6538), *Bacillus subtilis* (ATCC-6633), *Escherichia coli* (ATCC-25922), *Pseudomonas aeruginosa* (ATCC-15442), Resistant *Pseudomonas aeruginosa*(MIC-103), Methicillin Resistant *Staphylococcus aureus*(MIC-104), Resistant *Escherichia coli* (MIC-102) and Resistant *Streptococcus hemolyticus*(-MIC-101) were tested in this study. Fungal strains including *Aspergillus flavus*(FCBP-0064), *Mucor species* (FCBP-0300), *Aspergillus niger*(FCBP-0198), *Fusarium solani*(FCBP-0291) and *Aspergillus fumigatus* (FCBP-66) were used. Chloroquine-sensitive *Plasmodium falciparum* D6 strain (Sierra Leone PfD6), chloroquine-resistant *P. falciparum* W2 strain (Indochina PfW2) and *Leishmania tropica*kWh 23 were utilized.

2.4. Artemia salina eggs

Brine shrimp eggs, acquired from Ocean star International, USA has been utilized.

2.5. Animals

About 7 weeks old Balb/c mice, weighing ~25–30 g of either sex were used in the study. All animals were housed under standard 12-h light and dark and cycles with food and water provided ad libitum. Animals were acclimatized to the laboratory environment for 30 min before the experiment.

2.6. Ethical statement

After taking, written informed consent, blood was collected from two healthy female individuals (less than 30 years) by

venipuncture to isolate lymphocytes. Donors conferred that they were not recently exposed to drug treatment, smoking, radiation or any viral infection. International ethical guidelines were followed after approval by the Ethical Board of the Quaid-i-Azam University, Islamabad, Pakistan (Letter # BEC-FBS-QAU-042/2019). Guidelines for the care and use of laboratory animals narrated by National Institute of Health, USA were adhered with cautions to diminish animal distress. Study was conducted after approval of experimental protocol (Letter # BEC-FBS-QAU-067/2019) and animal use (Letter # BEC-FBS-QAU-089/2019) from the Institutional Animal Ethics Committee.

2.7. Preparation of extracts

Plant was recognized by its local name and was collected from Hunza valley, Baltistan in August 2018. The plant sample was identified and submitted under a voucher number PHM 512 to the Herbarium of Medicinal plants, Department of Pharmacy, Quaid-i-Azam University, Islamabad, Pakistan. Plant material was sorted to remove weeds and rinsed with tap water to eliminate any contamination or dust. It was then shade dried at ambient temperature with sufficient ventilation for a period of three weeks. Completely dried plant was pulverized by commercial miller to a fine powder, which was kept in airtight jars. Analytical grade solvents i.e., n-Hexane (NH), ethyl acetate (EA), methanol (M) and distilled water (DW) were used for extraction. Plant material was macerated with solvent (1:4) in Erlenmeyer flask (1000 ml) for three days at room temperature. Extraction was facilitated by intermittent sonication cycles in an ultra-sonic bath (25°C, 30 min) on daily basis. After the specified time period, filtration was done while marc was re-macerated using same solvent for 1 day followed by filtration. Obtained marc was macerated with the left three solvents i.e., EA, M and DW successively. Same conditions were applied each time. Filtration was carried out using muslin cloth and Whattman No. 1 filter paper. All filtrates of the same solvent were merged and concentrated using a rotary evaporator (R-210 Buchi, Flawil, Switzerland) at 60°C. Concentrated extract was further dried using vacuum oven (Yamato, Japan) at 45 °C and stored at −30°C till further use.

2.8. Phytochemical analysis

2.8.1. Total phenolic content

Folin-Ciocalteu (FC) reagent method was used to estimate total phenolic content (Fatima et al., 2015). An aliquot of 20 µl (4 mg/ml DMSO) of the extracts was transferred in the respective wells of 96 well plate followed by the addition of 90 µl of FC reagent. Then 90 µl of Na_2CO_3 was added to the reaction mixture and incubated for 30 min at 37°C. Absorbance was noted at 630 nm by microplate reader (Biotech USA, microplate reader Elx 800). Using gallic acid (3.125–25 µg/ml) as positive control a calibration curve was drawn. The assay was performed in triplicate and results were expressed in microgram gallic acid equivalent per milligram of the extract (µg GAE/mgE).

2.8.2. Total flavonoid content

Previously described aluminum chloride colorimetric method with slight modification was adopted (Ahmed et al., 2017). Briefly, 20 µl of each extract (4 mg/ml DMSO), 10 µl each of 10% $AlCl_3$, 1 M potassium acetate and 160 µl of DW were mixed in wells of 96 well plate. This reaction mixture was incubated for 30 min and read at 415 nm with the help microplate reader. Resultswere calculated in microgram quercetin equivalent per milligram of the extract (µg QE/mgE) at different concentrations of quercetin (40, 20, 10, 5, 2.5 and 0 µg/ml). Assay was run in triplicate.

2.8.3. RP-HPLC analysis

(1) *Detection of artemisinin and its derivatives*

Artemisinin and its analogs were quantified using previously defined protocols with minor modifications (Fatima et al., 2015). Each extract (10 mg/ml) was dissolved separately in HPLC grade methanol. All the solutions were sonicated, centrifuged and filtered through 0.2 µm sartolon polyamide membrane filter. Artemisinin standards (artesunate, artemether, dihydroadtemisinin and artemisinin) were prepared in HPLC grade methanol with the final concentration of 250 ppm and were eluted at flow rate of 1 ml per min with injection volume of 50µmµl using Agilent Chem station Rev. B.02-01-SR1 (260) and Agilent 1200 series binary gradient pump coupled with diode array detector (DAD). Reverse phase chromatographic analysis was carried out with a Zorbex-C8 analytical column (4.6 × 250 mm, 5 µm particle size), mobile phase A (acetonitrile) and mobile phase B (phosphate buffer) at gradient method of 0–3 min for 0–70% B, 3–7 min for 70–60% B, 7–10 min for 60–50% B and then 70% B until 30 min. The absorption of samples was recorded at 210 nm.

(2) *Detection of polyphenolic compounds*

RP-HPLC profiling was done for quantitative analysis of polyphenols using 8 standards by previously described procedure (Ahmed et al., 2017). HPLC grade methanol was used to extract the samples and re-filtered using 0.45 µm membrane filters (Milex-HV). The HPLC system was Agilent Chem station Rev. B.02-01-SR1 (260) and Agilent 1200 series binary gradient pump coupled with diode array detector (DAD). Analytical column Zorbex-C8 (4.6 × 250 mm, 5 µm particle size) with 50 µl of injection volume was used. Mobile phase consisted of acetonitrile-methanol–water-acetic acid in a ratio of 5:10:85:1 (solvent A) and acetonitrile-methanol-acetic acid in a ratio of 40:60:1 (solvent B). Gradient method was 0–20 min for 0–50% B, 20–25 min for 50–100% B and then isocratic 100% B until 30 min. Flow rate was maintained at 1 ml/min. The column was reconditioned for 10 min every time before next analysis. Polyphenols were identified by comparing retention time and UV–Vis spectra of chromatoghraphic peaks with reference standards at 257 nm (vanillic acid) and 279 nm (gallic acid, syringic acid, emodin), 325 nm (luteolin, ferulic acid, gentisic acid).

2.8.4. High resolution mass spectroscopy (HRMS)

Accurate mass measurements for molecular formula determinations were obtained on a ThermoVelos Pro electrospray ionization (ESI) hybrid ion trap-Orbitrap mass spectrometer (Thermo Fisher, Waltham, MA, USA). MS spectra were obtained using a ThermoVelos Pro-ESI ion trap mass spectrometer using collision-induced dissociation energy of 35 V. Spectra were collected between m/z of 0 and 2000 using XCalibur software (Thermo Fisher) (Lin et al., 2017).

2.9. Biological evaluation

2.9.1. Antioxidant potential of A. Brevifolia extracts

(1) *Percent free radical scavenging activity (FRSA)*

FRSA of the extracts was evaluated using methanol solution of DPPH (Ahmed et al., 2017, Baig et al., 2020). An aliquot of 10 µl of the extracts (4 mg/ml DMSO) were added to respective wells of 96 well plate. DPPH solution (190 µl) was then added in each

well followed by incubation for 1 h at 37°C in dark. Absorbance was noted at 517 nm using microplate reader. Ascorbic acid was used as positive control whereas DMSO was used as negative control. PercentFRSA was calculated according to the given formula;

$$Percent\ \ FRSA = \left[1 - \left(\frac{Absorbance\ \ of\ \ Sample}{Absorbance\ \ of\ \ Control}\right)\right] * 100$$

Extracts having FRSA ≥ 50% were further examined at lower concentrations of 200, 66.6, 22.22 and 7.4 μg/ml to evaluate their 50% inhibitory concentration (IC_{50}) in μg/ml. The assay was performed in triplicate.

(2) *Total antioxidant capacity*

Phosphomolybdenum based total antioxidant capacity was determined using ascorbic acid as positive control (Nasir et al., 2020). Briefly, 100 μl of each extract (4 mg/ml DMSO) was mixed with 900 μl of TAC reagent (0.6 M sulfuric acid, 28 mM sodium phosphate and 4 mM ammonium molybdate solution in water) in Eppendorf tubes followed by incubation in water bath at the temperature of 95°C for 90 min. Tubes were cooled to room temperature from which 200 μl of each sample was transferred to 96 well plate and absorbance was measured at 630 nm using microplate reader. The assay was done in triplicate. Antioxidant potential was measured in microgram ascorbic acid equivalent per milligram of the extract (μg AAE/mgE). DMSO was used as negative control.

(3) *Total reducing power*

Reducing power of the extracts was evaluated using standard potassium ferricyanide colorimetric assay (Fatima et al., 2015). Briefly, 200 μl of extract samples (4 mg/ml DMSO) was mixed with 400 μl each of phosphate buffer (0.2 M, pH 6.6) and 1% (w/v) potassium ferricyanide followed by an incubation at 50 °C for 20 min. After the addition of 200 μl of 10% (w/v) TCA, Eppendorf tubes were centrifuged at 3000 rpm for 10 min. About 150 μl of supernatant was transferred to respective wells of 96 well plate followed by the addition of 50 μl of 0.1% (w/v) $FeCl_3$. Absorbance was measure at 630 nm. Ascorbic acid served as positive control at 6.25–100 μg/ml final concentrations. DMSO was used as negative control. Assay was performed in triplicate. Results were expressed as μg AAE/mgE.

(4) *β-carotene scavenging activity*

Capability of extracts to inhibit the β-carotene bleaching was recorded (Majid et al., 2015). Reaction mixture was prepared by dissolving β-carotene (2 mg/ml), tween 80 (200 mg) and linoleic acid (20 mg) in 10 ml of chloroform. Afterwards, a uniform emulsion of β-carotene linoleate was prepared by evaporating the chloroform using vacuum followed by the addition of distilled water (50 ml). An aliquot of 30 μl of extract was mixed with 250 μl of β-carotene linoleate emulsion. Zero h reading was taken at 470 nm. Reaction mixture was kept at 45°C for 2 h and then final optical density was recorded. Catechin was used as positive standard whereas DMSO was used as negative control. Assay was performed in triplicate. Percent of inhibition of β-carotene bleaching was calculated using the underlying formula;

$$Percent\ \ of\ \ inhibition = \left[1 - \left(\frac{Aa(120) - Ac(120)}{Ac(0) - Aa(120)}\right)\right] * 100$$

where Aa(1 2 0) and A_C (1 2 0) are the absorbance of antioxidant and control, respectively taken after 2 h whereas aa (0) and Ac(0) are the zero h readings of antioxidant and control.

(5) *Iron chelating activity*

Procedure described by Majid et al. (2015)was followed. About 200 μl of extract sample, 100 μl of iron (II) chloride dihydrate (2.0 mM) and 900 μl of methanol were mixed carefully followed by an incubation period of 5 min. Reaction mixture was again incubated at 37°C for 10 min after the addition of 400 μl of ferrozine (5.0 mM). Spectrophotometry was performed at 562 nm. EDTA was used as positive standard. The assay was done in triplicate. Underlying formula was used to calculate the percent of chelating effect;

$$Percent\ \ of\ \ chelating\ \ effect = \left(\frac{Ac - As}{Ac}\right) * 100$$

where Ac and As are the absorbance of control and samples respectively.

2.9.2. Antimicrobial potential of A. brevifolia extracts

(1) *Antibacterial assay*

Previously described disc diffusion method with slight modifications was utilized to examine the antibacterial potential of extracts against nine bacterial strains (Zahra et al., 2017). An aliquot of 100 μl of inoculum with pre-adjusted seeding density was swabbed slowly in three different directions over the surface of nutrient agar media plates. Sterile filter paper discs loaded with 5 μl (20 mg/ml DMSO) of extracts were placed on the surface of the plates. Roxithromycin and cefixime loaded discs were utilized as positive control whereas DMSO infused disc was used as a negative control. After an incubation of 24 h at 37°C, zone of inhibition (ZOI) was measured using Vernier calliper. Minimum inhibitory concentration (MIC) was determined for the extracts showing zones greater than 12 mm by standard three-fold microbroth dilution method with concentration ranging from 200 to 7.40 μg/ml. An aliquot of 195 μl of bacterial culture (inoculum size ~5×10^4 CFU/ml) was added to each dilution followed by the incubation of plates for 30 min at 37°C. Zero h reading at 630 nm was noted using microplate reader. The plates were again incubated at 37°C for 24 h and absorbance was recorded. The difference of the two values of absorbance was found to determine net change in turbidity. Following formula was used to find out the percent of growth inhibition:

$$Percent\ \ of\ \ growth\ \ inhibition = \left[1 - \left(\frac{Turbidity\ \ of\ \ Test\ \ Sample}{Turbidity\ \ of\ \ Negative\ \ Control}\right)\right] * 100$$

Lowest concentration exhibiting ≥90% bacterial growth inhibition was declared as MIC. The assay was done in triplicate.

(2) *Antifungal assay*

Antifungal potential of extracts was assessed by disc diffusion method against five fungal strains(Nasir et al., 2017). Fungal spores were harvested in 0.02% Tween 20 solution. McFarland 0.5 turbidity standard was utilized to adjust turbidity. About 100 μl of fungal spore suspension was swabbed on SDA plates followed by the placement of the extract loaded sterile filter paper discs (5 μl; 20 mg/ml DMSO). Clotrimazole and DMSO impregnated disc were used as a positive and negative controls, respectively. Plates were then incubated for 24–48 h at 28°C. Diameter of ZOI around each disc was measured using Vernier calliper. Extracts producing ZOI ≥ 10 mm were screened to determine MIC at lower concentrations ranging from 200 to 7.4 μg/disc by standard disc diffusion method. Lowest concentration of the extract, which depicted a visible ZOI was considered as MIC.

2.9.3. Antiprotozoal potential of A. brevifolia extracts

(1) *Antileishmanial activity*

Previously described MTT assay with slight modifications was employed to evaluate the *in vitro*antileishmanial potential of extracts (Waseem et al., 2017). A 6–7 days incubated *L. tropica* promastigotes culture was used. Parasites were cultivated in RPMI 1640 Medium containing 100 IU/ml benzyl penicillin, 100 µg/ml streptomycin sulphate and 10% fetal bovine serum (FBS) at 24°C. About 180 µl of parasitic culture at a seeding density of 1×10^6 promastigotes/ml was transferred to respective wells of 96 well plate already containing 20 µl (100 µg/ml) of extracts (prepared in ≤1% DMSO in PBS). Amphotericin B (0.33 to 0.004 µg/ml) was used as positive control. DMSO (1%) in PBS was used as negative control. After incubation for 72 h at 24°C, 20 µl of sterilized MTT solution (4 mg/ml in distilled water) was added to each well and plates were incubated for 4 h at 24°C. Afterwards, supernatant was discarded carefully in order not to disturb the colored water insoluble formazan crystals, which were dissolved in 100 µl of DMSO and stabilized for 60 min. Absorbance was recorded at 540 nm using microplate reader. Following formula was used to determine percent of cytotoxicity;

$$Percent\ of\ cytotoxicity = 100 - \left[\left(\frac{Absorbance\ of\ Sample}{Absorbance\ of\ Control}\right) * 100\right]$$

Samples exhibiting >50% cell mortality were further analyzed at lower concentrations, i.e., 33.3, 11.1, 3.7 and 1.23 µg/ml. Table curve 2D v5.01 software was used to calculate IC_{50}.

(2) *Antimalarial activity*

Antimalarial activity of the theextracts was evaluated against the chloroquine sensitive and resistant strains of *P.falciparum*, i.e., D6 and W2 according to previously defined methodology (Kaou et al., 2008). Human erythrocytes were cultured in A+ blood and suspended in RPMI 1640 medium supplemented with HEPES (25 mM), 10% human serum and $NaHCO_3$ (25 mM). Strains were subjected to incubation in a humidified atmosphere of 5% CO_2 at 37°C. Parasitemia was maintained between 1 and 5% with non-parasitized blood for adjustment of instrument. Assay was executed in triplicate in 96 well plate containing 20 µl of respective extracts and 180 µl of parasite culture at 2% hematocrit and parasitemia. Extracts were tested at a concentration of 100 µg/ml. Chloroquine was used as positive whereas 1% DMSO in PBS was used as negative control. Plates were incubated for 48 h in a CO_2 atmosphere at 37°C. Later, parasitemia was evaluated through flow cytometry using hydroethidine. Plates were centrifuged. Supernatant was discarded and 200 µl of hydroethidine solution (0.05 mg/ml in PBS) was added. Plates were again incubated for 20 min at 37°C in the dark and then parasites were washed twice with PBS by centrifugation at 1890 rpm for 10 min. Parasites were suspended in 1 ml of PBS in the tubes for fluorescence activated cell sorter (FACS) analysis for determination of parasitemia. Following formula was utilized to calculate percent of parasitemia;

$$Percent\ of\ parasitemia = \left(\frac{Number\ of\ Infected\ Erythrocytes}{Total\ Number\ of\ Erythrocyes}\right) * 100$$

2.9.4. Cytotoxic potential of A. brevifolia extracts

(1) *Cytotoxicity against A. salina (Brine shrimps)*

Previously described lethality test was performed using 96 well plate against *A. salina* (Nasir et al., 2017). Shrimps were hatched after an incubation of 24–48 h, in simulated sea water (38 g/l) supplemented with dried yeast (6 mg/l), under light and warmth at 30–32°C. Two-fold serial dilutions of the extracts were prepared using ≤1% DMSO in sea water to get final concentrations of 200, 100, 50 and 25 µg/ml. Harvested mature phototropic nauplii (n = 10) in 150 µl of sea water were transferred to respective wells. A final volume of 300 µl was made using sea water. Doxorubicin at the concentrations of 10, 5, 2.5 and1.25 µg/ml, was used as positive control whereas 1% DMSO was used as negative control. Afterwards, plates were incubated at 37°C for 24 h. Dead nauplii were counted using inverted microscope. Percent of lethality was calculated with the help of following formula;

$$Percent\ of\ lethality = \left(\frac{Number\ of\ Dead\ Shrimps}{Total\ Number\ of\ Shrimps}\right) * 100$$

Extracts having inhibition greater than 50% were further examined at lower concentration to find median lethal dose (LD50) using graph pad prism 5 software.

(2) *Cytotoxicity against cancer cell lines*

The *in vitro* cytotoxicity against different cancer cell lines including HepG2, A2780, THP-1, MCF-7, HT-29 and DU-145 was evaluated using MTT assay (Waseem et al., 2017). Complete growth medium, RPMI-1640 (pH 7.4) supplemented with 10% v/v HIFBS and 2.2 g/l $NaHCO_3$ was used for culturing cancer cell lines in a humidified CO_2 incubator (5% CO_2) at 37°C. Briefly 190 µl of harvested culture with seeding density of 1×10^5 cells/ml, was added to respective wells of 96 well plate followed by the addition of 10 µl of the *A. brevifolia* extracts (1% DMSO in PBS) with a final concentration of 20 µg/ml. Cisplatin, 5-flourouracil, vincristine and doxorubicin (4 mg/ml DMSO) were used as positive while 1% DMSO in PBS was used as negative control. After an incubation at 37°C in a CO_2 (5%) humidified incubator for 72 h, MTT assay was performed as described in Section (2.9.3.1). Extracts exhibiting >50% activity were further screened at lower concentrations, i.e., 10, 5, 2.5 and 1.25 µg/ml. Assay was repeated thrice. IC_{50} was calculated using table curve 2D v5.01 software.

(3) *Cytotoxicity against isolated lymphocytes*

Previously described protocol with slight modifications was used for lymphocytes isolation (Waseem et al., 2017). About 3 ml of blood was collected from healthy volunteer after venipuncture and diluted (1:1) with PBS. After layering over 2 ml of Histopaque-1077, blood was centrifuged at 800*g* for 20 min. Buffy coat, formed in the center, was aspirated in 5 ml of PBS and centrifuged for 4 min at 350 rpm. Growth medium, RPMI-1640 (1 ml) was used to suspend the pellet and cell density was adjusted to get 1×10^5 cells/ml. For cytotoxicity determination, 20 µl of extracts at the final concentration of 20 µg/ml was incubated with 180 µl of lymphocyte with a seeding density of 1×10^5 cells/ml, at 37°C for 24 h in humidified 5% CO_2 incubator. Vincristine (4 mg/ml) or 1% DMSO in PBS were used as positive and negative controls, respectively. Afterwards, previously described MTT assay (2.9.3.1) was performed.

2.9.5. Genotoxicity assays

(1) *Comet assay*

Comet assay method with slight modifications was employed for genotoxicity evaluation of the extracts (Kazmi et al., 2018). Briefly, cancer cell lines were cultured in DMEM medium (with low glucose and 4 mM l-glutamine) supplemented with 10% v/v HIFBS, 100 U/ml benzyl penicillin and 100 µg/ml streptomycin sulphate. About 180 µl of monolayer respective cell lines cultures were seeded at a density of 5×10^4 cells/well and allowed to adhere overnight under an atmosphere of 5% CO_2 at 37°C. After an incubation of 24 h, cells were treated with 20 µl of the extracts with a concentration of 100 µg/ml and incubated again for 72 h

under the same conditions. Cisplatin at the final concentration of 0.5 μg/ml was used as positive control. Later on, the cells were trypsinized using a mixture of EDTA and trypsin and centrifuged at 100*g*, for 5 min at a temperature of 4°C in 150 μl of molten 0.5% LMPA. The cell suspensions were rapidly spread on microscopic slides pre-coated with 85 μl of 1% NMPA and covered with cover-slip (25 mm × 25 mm). Agarose was solidified by keeping the slides at 4°C for 5 min. Coverslips were detached carefully and another layer of 75 μl LMPA was added. Slides were exposed to lysis solution (2.5 M NaCl, 0.1 M Na_2-EDTA, 0.01 M trisHCl,1% Triton X-100 and 10% DMSO) for a period of 2 h at 4°C. Later, slides were kept in an electrophoresis tank containing alkaline electrophoresis buffer (pH 13) and allowed to sit in for 20 min for unwinding the DNA. Slides were then electrophoresed for a period of 20 min (300 mA; 25 V). Tris buffer (pH 7.5) was used to neutralize the alkali. Slides were stained with 80 μl 1X ethidium bromide and left for 7 min. Chilled distilled water was used to remove the excess stain. Coverslip was then placed and slides were examined immediately using fluorescent microscope. Images were scored using CASP 1.2.3.b software. For each sample, nearly 50–100 cells were observed for comet length (CL), head length (HL), percent of DNA in head as well as tail, tail length (TL) and tail moment (TM) of nuclei for each sample.

(2) *Micronucleus assay*

Micronucleus assay with cytokinesis block was conducted according to previously described procedure (Tsuboy et al., 2007). Cancer cell lines were cultivated as monolayer cultures in DMEM media supplemented with 10% HIFBS, 100 U/ml benzyl penicillin and 100 μg/ml streptomycin sulphate and incubated under humidified atmosphere of 5% CO_2 at 37°C. Cell suspensions at a density of 2.5 × 10^5 cells were grown in 25 cm^2 flasks. After 48 h, observing a confluence of 60–70%, medium was removed and cells were treated with extracts at a concentration of 100 μg/ml. For antimutagenicity testing, the cultures were simultaneously exposed to the combination of cisplatin and extracts or cisplatin alone (at the final concentration of 0.5 μg/ml). After 24 h of incubation, cells were again incubated with media supplemented with cytochalasin B having a final concentration of 6 μg/ml for a period of 24 h. Later on, cells were exposed to cold hypotonic solution of KCL (5.6 g/l) and centrifuged at 800 rpm for 8 min. Cell were fixed using acetic acid:methanol (1:3) and 2 drops of formaldehyde. Slides were coded and stained using 5% aqueous Giemsa solution for a period of 15 min. About 1000 binucleated cells (BN) per culture with intact cytoplasm were scored for the incidence of percent micronucleus formation (%MN). Nuclear division index (NDI) was calculated for each experimental point.

(3) *Chromosomal aberration assay*

Chromosomal aberration assay was performed according to previously described protocol to detect the potential anticlastogenic effects of *A. brevifolia*using cancer cell lines with a seeding density of 3.8 × 10^5 cells/dish (Imreova et al., 2017). When a confluency of 70% was observed, seeded cells were incubated with the *A. brevifolia* extracts at a concentration of 100 μg/ml for 24 h. Later on old medium was replaced with fresh medium while positive control dishes were treated with the media containing mutagen cisplatin (0.5 μg/ml). Cells were cultivated for 42 h. An intact control group was mounted without extract. Colchicine at a concentration of 0.75 μg/ml was added 3 h before the end of incubation. Cells were counted before karyological processing. Slides were stained using 10% aqueous Giemsa solution for 10 min. Microscopic examination was executed to evaluate the chromosomal aberrations. About 100 metaphases were analyzed for each sample. Structural aberrations including chromatid, *iso*-chromatid, breaks and exchanges were observed.

2.9.6. In vitro anti-inflammatory activity

Nitric oxide scavenging potential of extracts was assessed following the protocol narrated by Majid et al. (2015) with minor modification. Equal volumes of 0.1% napthylenediamine (1 mg/ml) in distilled water and 1% of sulphanilamide (10 mg/ml) in 5% phosphoric acid were added to prepare Griess reagent. About 100 μl of both, samples and sodium nitroprusside (10 mM), were mixed followed by the addition of 1 ml of the Griess reagent and incubation at room temperature for 3 h. Absorbance was read at 546 nm using ascorbic acid as a positive control. Following formula was used for determining the percent of nitric oxide radical formation inhibition.

$$Percent\ \ of\ \ inhibition = \left(\frac{Absorbance\ \ of\ \ Control - Absorbance\ \ of\ \ Sample}{Absorbance\ \ of\ \ Control}\right) * 100$$

2.9.7. In vivo anti-inflammatory activity

(1) *Experimental design for in vivo anti-inflammatory assays*

About 7 weeks old Balb/c mice (n = 5) weighing ~25–30 g of either sex were used in the study. Animals were housed in aluminum cages under hygienic conditions (12 h light/dark cycle, 25 ± 1°C temperature) at primate Facility of Quaid-i-Azam University Islamabad, Pakistan. All the animals were supplied with standard chow feed along with water ad libitum prior to use in experiments. Mice were randomly divided into 11 groups, where group I-III were designated as Normal, Vehicle and Positive control groups which received normal saline only, 10% DMSO in 0.75% carboxymethyl cellulose solution and ibuprofen (10 mg/kg), respectively. Group IV-XI were treatment groups, which were designated as NHL, NHH, EAL, EAH, ML, MH, DWL and DWH, where L and H represents low (150 mg/kg body weight) and high dose (300 mg/kg body weight), respectively. Dose was administered orally. Carrageenan suspension (0.9% *w*/*v* in normal saline) was used to induce hind paw edema whereas 0.2 ml of 6% croton oil in diethyl ether was used to induce anal edema.

(2) *In vivo carageenan induced paw edema inhibition assay*

Anti-inflammatory prospects of the extracts were determined with the help of Carrageenan-induced hind paw edema model described by Majid et al.(2018)with slight modifications. Extracts were administered 60 min before injecting 150 μl of carrageenan suspension in planter aponeurosis. Hind paw edema volume (mm) was immediately recorded by measuring paw circumference after injection (zero h) and was noted again after time interval of 1, 2, 3 and 4 husing Plethysmometer (Ugo Basile 7140, Italy). Results were calculated as:

$$Percent\ \ of\ \ inhibition = \left(\frac{Control\ \ Animal\ \ Edema\ \ Vol - Test\ \ Animal\ \ Edema\ \ Vol}{Control\ \ Animal\ \ Edema\ \ Vol}\right) * 100$$

(3) *In vivo croton oil induced anal edema inhibition*

Previously described noninvasive protocol was used to assess the croton oil induced edema response on anus of test animals (Majid et al., 2018). Cotton swab soaked with inducer was rubbed for 10 sec on anus of mice around 60 min after the oral administra-

tion of specified doses. Readings were noted for 1st, 2nd, 3rd and 4th h using Vernier calliper. Anti-inflammatory potential was determined by reduction in anal edema by comparing it with positive control.

$$Percent\ of\ inhibition = \left(\frac{Control\ Animal\ Edema\ Vol - Test\ Animal\ Edema\ Vol}{Control\ Animal\ Edema\ Vol}\right) * 100$$

2.9.8. Enzyme inhibition assays

(1) *α-amylase inhibition assay*

Antidiabetic potential of the extracts was determined through α-amylase inhibition assay following standard protocol with slight modification (Ahmed et al., 2019). Reaction mixture containing 15 µl of PBS (pH 6.8), 25 µl of α-amylase enzyme (0.14 U/ml) followed by the addition of 10 µl extract (4 mg/ml DMSO) and 40 µl of starch (2 mg/ml in potassium phosphate buffer) was incubated for 30 min at 50 °C. Aliquot of 20 µl of 1 M HCl was then added to respective wells of 96 well plate to stop the reaction. Finally, 90 µl of iodine reagent (5 mM iodine, 5 mM potassium iodide) was added. Acarbose solution and DMSO were added to the positive and negative control wells instead of extracts whereas blank was prepared without test samples and amylase enzyme. The absorbance was noted at 540 nm using microplate reader. IC_{50} was determined for the samples. Percent of inhibition was calculated with the help of given formula:

$$Percent\ of\ inhibition = \left(\frac{Absorbance\ of\ Sample - Absorbance\ of\ Negative\ Control}{Absorbance\ of\ Blank - Absorbance\ of\ Negative\ Control}\right) * 100$$

(2) *α-glucosidase inhibition assay*

Previously described procedure was employed for evaluating the α-glucosidase inhibitory potential of the samples (Ovais et al., 2018). An aliquote of 25 µl of p-nitrophenyl-D-glucopyranose (substrate) solution was added into respective wells of 96 well plate along with 69 µl of 50 mM phosphate buffer (pH 6.8). Later, 5 µl of eachextract (4 mg/ml DMSO) and 1 µl of enzyme (3 units/ml in 50 mM phosphate buffer; pH 6.8) were added. Initial reading at 405 nm was taken immediately using microplate reader. Plate was then incubated at 37 °C for 30 min. After incubation, 100 µl of $NaHCO_3$ solution (0.2 M) was added to stop the reaction and another reading was taken at 405 nm using microplate reader. Procedure was repeated for negative and positive controls where the extracts was replaced by DMSO and acarbose, respectively. Percent of inhibition of the enzyme activity was calculated using the following formula:

$$Percent\ of\ inhibition = \left(\frac{Absorbance\ of\ Control - Absorbance\ of\ Sample}{Absorbance\ of\ Control}\right) * 100$$

Samples, which depicted >50% inhibition in initial screening were further analyzed at lower concentration to find IC_{50}.

2.10. Statistical analysis

Data obtained in this study was presented as mean ± SD. The results obtained for phytochemical and cytotoxic assays were analyzed statistically using computer software Statistix 8.1. Significant differences among the results obtained were calculated by Tukey's multiple comparisons. Statistical significance was set at $p < 0.05$. Graphs were generated using software GraphPad Prism 5.

3. Results

3.1. Percent extract recovery

Percent recovery of extracts prepared using solvents of successive polarity has been summarized in the Table 1. Highest extraction recovery was observed by DW extract (5.95% w/w) followed by M (4.25% w/w) and EA (2.75% w/w) extracts. The lowest percent yield (1.5% w/w) was obtained in NH solvent.

3.2. Phytochemical analysis

3.2.1. Total phenolic content estimation

Total phenolic content of the extracts were calculated by calibration curve, y = 0.0943x-0.0661, R^2 = 0.9906 (Table 4).M extract depicted the maximum ($p < 0.05$) phenolic content, followed by DW and EA extracts, respectively. Minimum phenolic content was found in NH extract. Phenolic content decreased in extracts in following trend: M > DW > EA > NH.

3.2.2. Total flavonoid content estimation

Total flavonoid content are expressed in µg QE/mgEand calculated by calibration curve y = 0.0649x-0.0403, R^2 = 0.9927(Table 4). Highest flavonoids ($p < 0.05$) were found in M extract followed by DW and EA extracts, respectively. Lowest flavonoids were quantified in NH extract.

3.2.3. RP-HPLC analysis

(1) *Detection of artemisinin and its derivatives*

RP-HPLC analysis of *A. brevifolia* extracts was conducted to detect and quantify artemisinin and analogues (Table 2, Fig. 1). EA extractdepicted maximum quantities of artemisinin (50.7 ± 0. 01 µg/mgE), DH artemisinin (895 ± 0.03 µg/mgE), artesunate (155 ± 0.20 µg/mgE) and artemether (81.4 ± 0.3 µg/mgE). All these sesquiterpenes were found in NH extract as well, with maximum quantity of DH artemisinin, i.e., 643 ± 0.19 µg/mgE. M extract was found deficient of artemisinin only. None of the standard compounds were detected in DW extract.

(2) *Detection of polyphenolic compounds*

Quantification of polyphenolics as well as chromatographic fingerprinting of bioactive samples was done by RP-HPLC profiling using 8 standards (Fig. 2a). Quantities determined have been presented in Table 2. Significant quantities (µg/mgE) of vanillic acid (0.4 ± 0.01), syringic acid (0.1 ± 0.0), emodin (1.4 ± 0.13) and luteolin (0.7 ± 0.02) were retrieved in EA extract. A significant amount

Table 1
Percent recovery of *A.brevifolia* extracts using solvents of successive polarity.

S. No.	Solvent Code	Polarity Index	Extract Yield (%)
1	NH	0	1.5^{d}
2	EA	4.4	2.75^{c}
3	M	5.1	4.25^{b}
4	DW	9	5.95^{a}

Values are presented as mean from triplicate investigation. Means with different superscript (a–d) letters in the column are significantly ($p < 0.05$) different from one another. NH: n-hexane, EA: Ethyl acetate, M: Methanol, DW: Distilled water.

Table 2
RP-HPLC-DAD analysis of *A.brevifolia* extracts for their sesquiterpenes and polyphenolic composition.

Standards (µg/mg of the extract)	Retention time (min)	Detection wavelength (nm)	Samples			
			NH	EA	M	DW
Artemisinin and its analogues quantified in *A.brevifolia* extracts						
Artesunate	6.7	210	34.7 ± 0.01[b]	155 ± 0.20[a]	4.3 ± 0.07[c]	—
DH Artemisinin	9.3	210	643 ± 0.19[b]	895 ± 0.03[a]	63.7 ± 0.04[c]	—
Artemisinin	12.9	210	15.2 ± 0.11[b]	50.7 ± 0.01[a]	—	—
Artemether	20.9	210	49.2 ± 0.31[b]	81.4 ± 0.3[a]	9.68 ± 0.10[c]	—
Phenolic composition (µg/mg of the extract) of *A. brevifolia* extracts						
Vanillic acid	9.517	257	***	0.4 ± 0.01[a]	—	—
Gallic acid	3.434	279	***	—	1.9 ± 0.03[a]	0.1 ± 0.02[b]
Syringic acid	9.515	279	***	0.1 ± 0.0 [a]	—	—
Emodin	27.844	279	***	1.4 ± 0.13 [a]	—	—
Luteolin	18.372	325	***	0.7 ± 0.02[a]	—	—

Values are presented as mean ± SD from triplicate investigation. Means with different superscript (a–c) letters in the row are significantly ($p < 0.05$) different from one another. —: not detected, ***: not evaluated, NH: n-hexane, EA: Ethyl acetate, M: Methanol, DW: Distilled water.

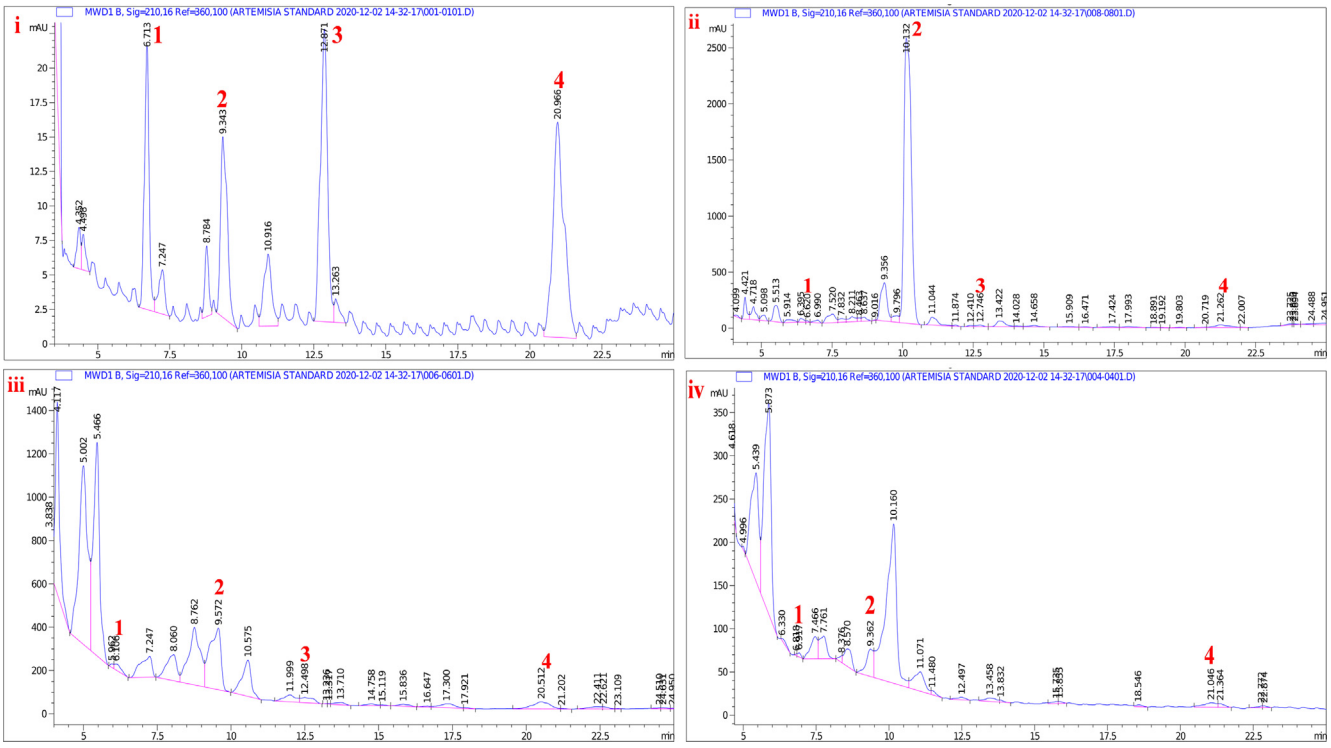

Fig. 1. RP-HPLC chromatograms of *A. brevifolia* extracts for artemisinin and its derivatives. i: standard compounds, ii: NH, iii: EA and iv: M extracts of *A. brevifolia* showing the presence of artemisinin and derivatives. 1: artesunate, 2: dihydro artemisinin, 3: artemisinin, 4: artemether. NH: n-Hexane, EA: Ethyl acetate, M: Methanol, DW: Distilled water.

of gallic acid has been quantified in M and DW extracts, i.e., 1.9 ± 0. 03and 0.1 ± 0.02 µg/mgE, respectively (Fig. 2b).

3.2.4. High resolution mass spectroscopy

Polar extracts were selected for HRMS and their spectrum results are as shown in Fig. 3. Total 40 compounds were detected where M contained 25 compounds eluted between 0.38 and 8.56 min (Table 3). Of these 25 compounds, there were caffeoylquinic acid derivatives, cinnamic sucrose esters, esterified fatty acid, flavonoid glycosides, lignan glycosides, sesquiterpenoids, steroid, heneicosane derivative and sugar molecules. A single glycon part of a glycoside was also detected. DW extract had 15 compounds including flavonoid glycosides, caffeoylquinic acid derivatives, jasmonic acid, eudesmanegluscoside, neolignans glucoside, quinones, sesquitepenoid derivative, triterpene derivative and steroid (cyasterone). Identification of these moieties was based on comparison of their relative retention times and mass spectra with those obtained from authentic sample literature survey.

3.3. Biological evaluation

3.3.1. Antioxidant potential of A. brevifolia extracts

3.3.1.1. Free radical scavenging assay. Significant percent scavenging activity of *A. brevifolia* extracts was assessed by the discoloration of DPPH solution. The M and DW extracts depicted maximum ($p < 0.05$) scavenging potential (Table 4). EA did not exhibit any significant scavenging activity whereas minimal scavenging activity was shown by NH extract. IC_{50} of ascorbic acid was found to be 21.8 µg/ml.

3.3.1.2. Determination of total antioxidant capacity. Total antioxidant capacity of the extracts were calculated by calibration curvey = 0.0268x − 0.062, R^2 = 0.9882 (Table 4).It was observed

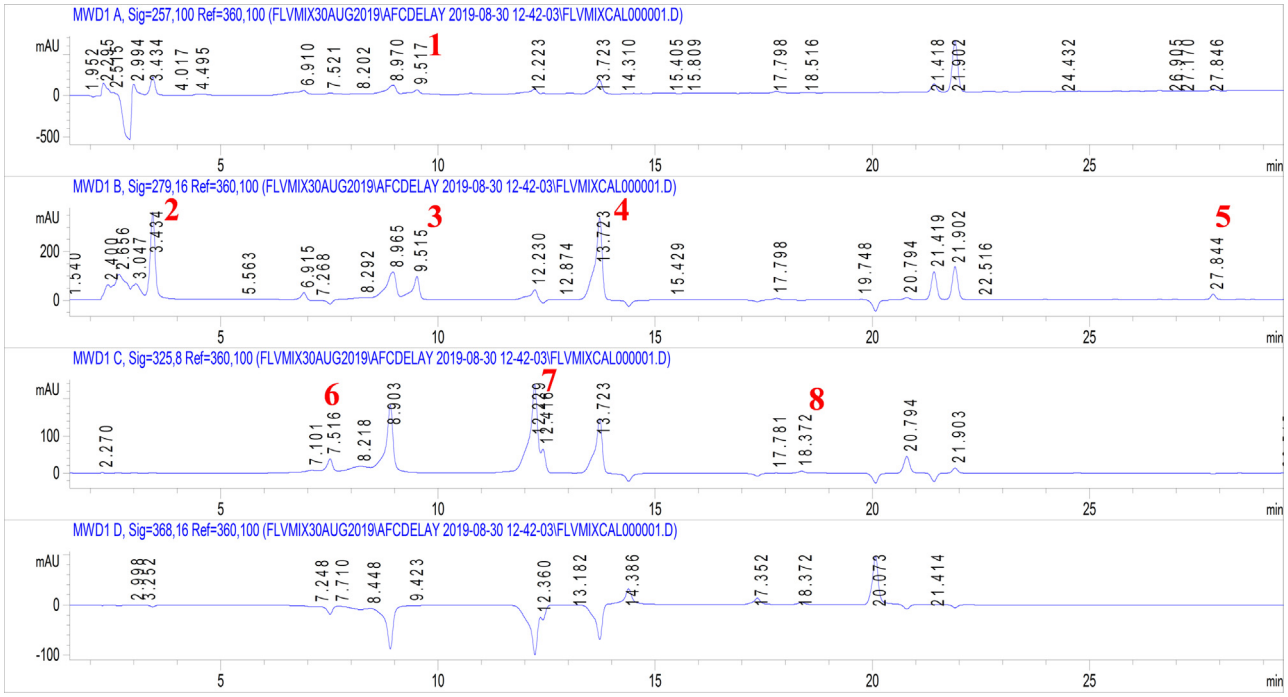

Fig. 2a. RP-HPLC chromatograms for standard mixture of polyphenolic compounds. 1: vanillic acid, 2: gallic acid, 3: syringic acid, 4: coumaric acid, 5: emodin, 6: gentisic acid, 7: ferulic acid, 8: luteolin.

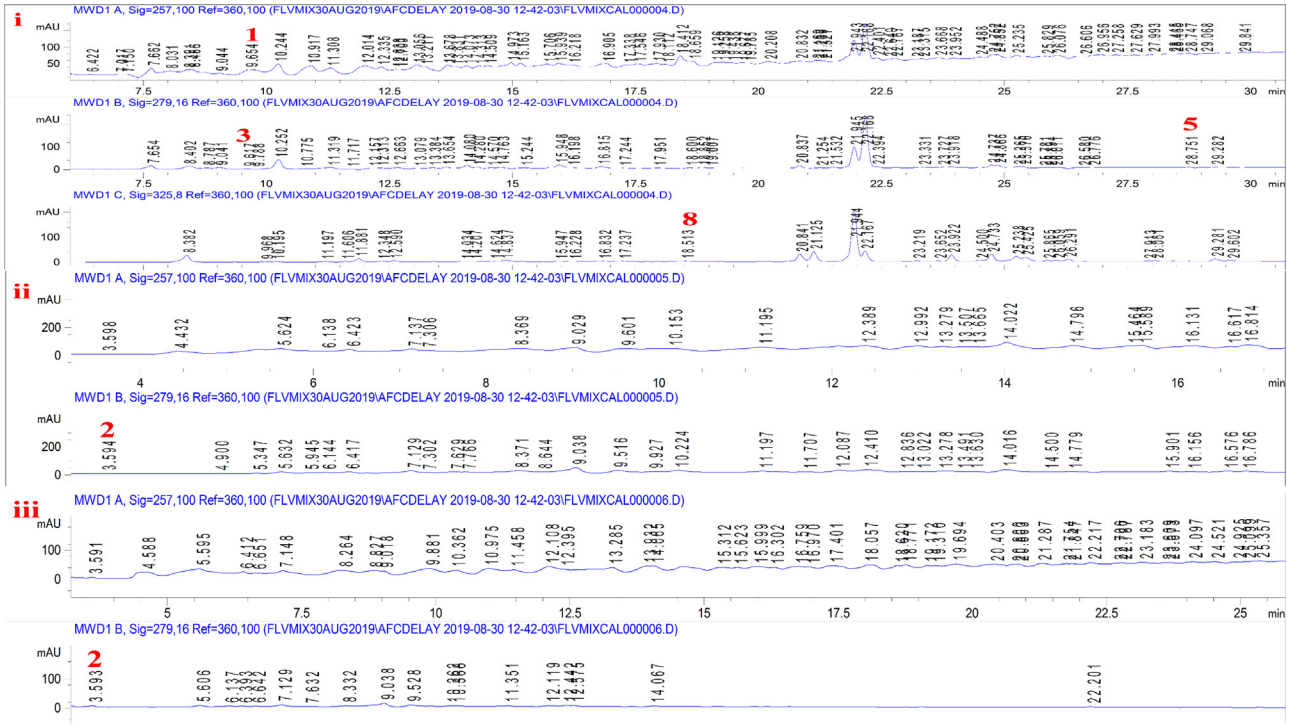

Fig. 2b. RP-HPLC chromatograms of *A. brevifolia*extracts. i: EA, ii: M, and iii: DW extracts of *A. brevifolia* showing the presence of polyphenolic compounds including 1: vanillic acid, 2: gallic acid, 3: syringic acid, 5: emodin, and 8: luteolin. EA: Ethyl acetate, M: Methanol, DW: Distilled water.

that highest antioxidant capacity ($p < 0.05$) was depicted by M extract while NH exhibited minimum capacity. Total antioxidant capacity of *A. brevifolia* extracts was found to decrease in the following order M > DW > EA > NH.

3.3.1.3. Determination of total reducing power. Total reducing power of the extracts were calculated by calibration curvey = 0.0284x + 0. 0247, R^2 = 0.9965 (Table 4). Assay results showed that M extract exhibited maximum ($p < 0.05$) reduction potential (112.3 ± 1.2 µg

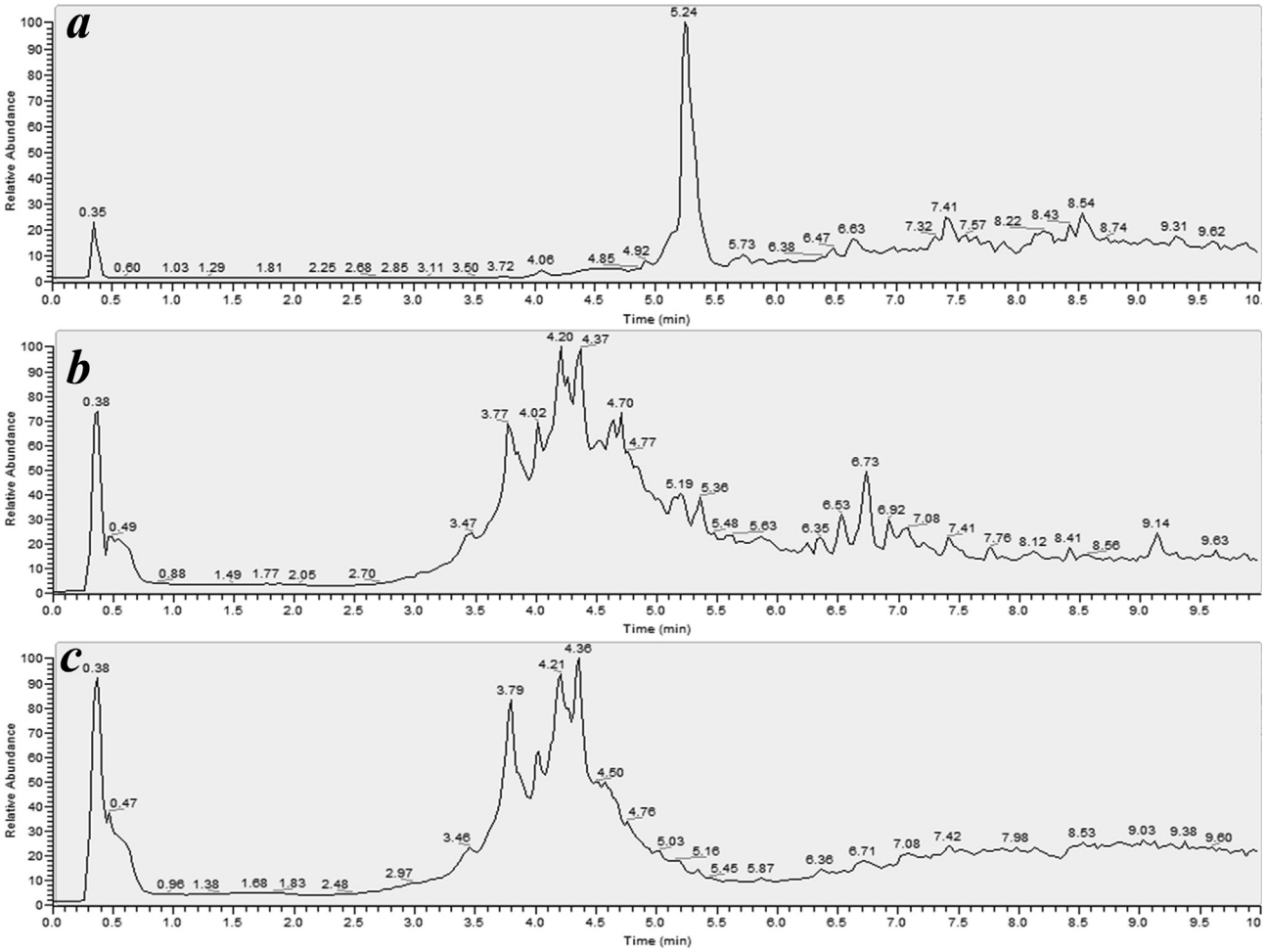

Fig. 3. Chromatograms of HRMS spectrum of *A. brevifolia*extracts. a: negative mode of reserpine, b: M, c: DW extracts of *A. brevifolia*. RT: retention time, HRMS: high resolution mass spectroscopy The standard reserpine gave $[M-H]^+$= 607.2652 at RT = 5.24 with molecular formula = $C_{33}H_{40}N_2O_9$,. X-axis represent time (minute) while Y-axis represents relative abundance. M: Methanol, DW: Distilled water.

AAE/mgE). DW extract also exhibited significantTRP followed by EA extract. Least TRP was manifested by NH extract, i.e., 16.6 ± 0. 6 μg AAE/mgE.

3.3.1.4. β-carotene scavenging activity. It is quite evident from the results that M extract showed the minimum IC_{50} value, i.e., 45.44 ± 1.23 μg/ml, as compared to other samples (Table 4). DW also exhibited strong antioxidant potential. Non-polar extracts, i.e., NH and EA exhibited an IC_{50} greater than 200 μg/ml. Catechin was used as a positive control, which gave an IC_{50} value of7.87 ± 0 .15 μg/ml.

3.3.1.5. Iron chelating activity. Minimum IC_{50} values for iron chelation (28.21 ± 1.18 and 45.33 ± 2.06 μg/ml) were demonstrated by M and DW extracts ($p < 0.05$), respectively(Table 4).. Herein, EA and NH extracts also exhibited a moderately significant activity, i.e., IC_{50} 139.45 ± 0.97 and 165.74 ± 2.76 μg/ml. Iron chelation potential of M extract was comparable to that exhibited by EDTA (18.85 ± 1.53 μg/ml; positive control).

3.3.2. Antimicrobial potential of A. brevifolia extracts

(1) *Antibacterial assay*

Results clearly depict that EA extract was found remarkably active ($p < 0.05$) against all the tested bacterial strains (Table 5). Maximum activity was found against *E. coli*, *B. subtilis*, *P. aeruginosa* and MRSA (MIC = 22.22 μg/ml). NH extract also demonstrated toxicity against all bacterial strains except Resistant *S. hemolyticus*.M extract showed maximum antibacterial activity against *E.coli* (MIC 22.22 μg/ml), *P. aeruginosa,* Resistant *P. aeruginosa* and MRSA (MIC 66.66 μg/ml). DW was active against *E. coli*, and *P. aeruginosa* (MIC 66.66 and 200 μg/ml, respectively). DMSO did not show any activity.

(2) *Antifungal assay*

EA extract exhibited significant ($p < 0.05$) antifungal potential against *F. solani*and *A. fumigatus* with MIC values of 66.66 and 22.22 μg/ml, respectively (Table 5). M extract also demonstrated activity against*A. flavus* and *A. fumigatus,* MIC = 66.66 μg/ml. A moderately significant activity against *F. solani,* with an inhibition zone of 10 ± 0.67 mm was exhibited by DW extract. NH extract did not show any activity. DMSO was also found inactive.

3.3.3. Antiprotozoal potential of A. brevifolia extracts

(1) *Antileishmanial activity*

It is quite evident from the results that NH and EA extracts demonstrated a significant ($p < 0.05$) *antileishmanial* potential with IC_{50} values of 13.91 ± 0.04 and 15.40 ± 0.09 μg/ml, respectively (Fig. 4). M and DW extracts also exhibited an inhibition of 48.57 ± 1.21 and 26.56 ± 0.41%, respectively. Amphotericin B gave an IC_{50} value of 0.01 μg/ml while no activity was observed with DMSO.

Table 3
Compounds identified in methanol and distilled water extracts of *A. brevifolia*.

S. No.	R.T.	$[M-H]^+$	M.F.	Compounds	Chemical Class
Methanol extract					
1	0.38	529.1340	$C_{26}H_{25}O_{12}$	1,3-Di-O-caffeoy quinic acid: Me-ester	Caffeoylquinic acid derivatives
2	0.49	515.1189	$C_{25}H_{24}O_{12}$	1,3-Di-O-caffeoylquinic acid	Caffeoylquinic acid
3	0.88	517.1561	$C_{22}H_{30}O_{14}$	1′-O(4-hydroxy-3-methoxy-cinnamoyl) sucrose	Cinnamic sucrose esters
4	1.49	517.1556	$C_{22}H_{30}O_{14}$	3′-O(4-hydroxy-3-methoxy-E-cinnamoyl) sucrose	Cinnamic sucrose esters
5	1.77	517.1556	$C_{22}H_{30}O_{14}$	3′-O(4-hydroxy-3-methoxy-Z-cinnamoyl) sucrose	Cinnamic sucrose esters
6	2.05	517.1561	$C_{22}H_{30}O_{14}$	6-O(4-hydroxy-3-methoxy-cinnamoyl) sucrose	Cinnamic sucrose esters
7	2.70	489.1969	$C_{22}H_{34}O_{12}$	2,4,7-decatrienoic acid glucopyranosyl (1 → 2) β–D- glucopyranosyl ester	Esterified fatty acid
8	3.47	563.1401	$C_{26}H_{28}O_{14}$	Apigenin 7-glycoside: 7-O-[β -D-Apiofuranosyl-(1 → 2) β–D-glucopyranoside	Flavonoid glycoside
9	3.77	563.1398	$C_{26}H_{28}O_{14}$	Apigenin 7-glycoside: 7-O-[β -D-Apiofuranosyl-(1 → 6) β–D-glucopyranoside	Flavonoid glycoside
10	4.02	577.1558	$C_{27}H_{30}O_{14}$	Apigenin 4′-7-diglycoside: 4-O-α-L-Rhamnopyranoside, 7-O-β-D-glucopyranoside	Flavonoid glycoside
11	4.20	515.1182	$C_{25}H_{24}O_{12}$	6-C- β-D-glucopuranosyl-4′,5,7-trihydroxyflavone:2″,6″-Di-Ac	Flavonoid glycoside
12	4.37	549.1964	$C_{27}H_{34}O_{12}$	2,7′-cyclo-2′,9-epoxy-8,8′-lignan-3,3′,4,4′,5,5′,9-heptol tetra Me ether, 9′-O- β-D-xylopyranoside	Lignan glycoside
13	4.51	563.2126	$C_{28}H_{36}O_{12}$	2,2′-*cyclo*-8,8′-lignan-3,3′,4,4′,5,5′,8-heptol,4′,5′-methylene, 3,3′,4-tri Me ether, 5-O-β-D-glucopyranoside	Lignan glycoside
14	4.62	563.2124	$C_{28}H_{36}O_{12}$	1-(3,5-dihydroxylphenyl)-2-(4-hydroxyphenyl)ethylene: 3,5-Di-Me ether, 4′-O-[α-L-rhamnopyranosyl-(1 → 6)- β-D-glucopyranoside]	Hydroquinone glucose
15	4.70	563.2122	$C_{28}H_{36}O_{12}$	1,(3,5-dihydroxyphenyl)-2-(4-hydroxyphenyl)ethylene: 3,4′-Di-Me ether, 5-O-[α-L-rhamnopyranosyl-(1 → 6)- β-D-glucopyranoside]	Glycone part of a glycoside
16	4.77	563.2122	$C_{28}H_{36}O_{12}$	4,7′-Epoxy-3,8′-lign-7-ene-3′,4′,5,5′,9,9′-hexol: (7E,7′R,8′S)-form, 3′,4′,5,5′-Tetra-Me ether, 9-O-β-D-glucopyranoside	Lignan glycoside
17	5.15	563.2122	$C_{28}H_{36}O_{12}$	7,9′-Epoxy-8,8′-lignan-3,3′,4,4′,9-pentol: (7R*,8S*,8′S*)-form, 3,3′-Di-Me ether, 4-O-[6-O-acetyl-β-D-glucopyranoside]	Lignan glycoside
18	5.36	561.2696	$C_{30}H_{42}O_{10}$	10,11-Epoxy-1,2,3,5,8-pentahydroxy-7(14)-bisabolen-4-one: 2,5,8-Triangeloyl	Sesquiterpenoid
19	5.45	561.2700	$C_{30}H_{42}O_{10}$	11,13-Epoxy-4,8,9-trihydroxy-3-oxo-10(14)-oplopen-12-oic acid: (8α,9β)-form, 8-(3-Methyl-2-pentenoyl), 9-(3-methylpentanoyl), 4-Ac, Me ester	Sesquiterpenoid
20	5.63	561.2699	$C_{30}H_{42}O_{10}$	1,3,4,5,8,10-Hexahydroxy-7(14),11-bisaboladien-2-one: 1,4,8-Triangeloyl	Sesquitepenoid
21	6.53	579.2833	$C_{30}H_{44}O_{11}$	1,3,4,5,8,10,11-Heptahydroxy-7(14)-bisabolen-2-one: 1,4,8-Triangeloyl	Sesquitepenoid
22	6.73	555.2833	$C_{28}H_{44}O_{11}$	7(14)-Bisabolene-1,2,3,4,5,8,10,11-octol: (1α,2α,3β,4α,5α,6αH,8ξ,10ξ)-form, 11-Me ether, 2,8-diangeloyl, 5-Ac	Sesquitepenoid
23	7.08	579.3381	$C_{28}H_{52}O_{12}$	Sucrose: Monohexadecanoyl	Disaccharide
24	7.41	521.3115	$C_{29}H_{46}O_8$	22,26-Epoxy-2,3,14,20,24,26-hexahydroxystigmast-7-en-6-one	Steroid
25	8.56	499.3638	$C_{28}H_{52}O_7$	Tetrahydro-4-hydroxy-6-(2,4,6-trihydroxyheneicosyl)–2H-pyran-2-one: (2′R*,4S*,4′S*,6R*,6′S*)-form, 2′-Ac	Heneicosane derivatives
Distilled water extract					
1	0.38	563.1396	$C_{26}H_{28}O_{14}$	Apigenin 7-glycosides: 7-O-[β-D-Apiofuranosyl-(1 → 2)-β-D-glucopyranoside]	Flavone glycoside
2	0.47	515.1189	$C_{25}H_{24}O_{12}$	1,3-Di-O-caffeoylquinic acid	Caffeoylquinic Acid Derivatives
3	1.68	353.0871	$C_{16}H_{18}O_9$	1-O-Caffeoylquinic acid	Caffeoylquinic Acid Derivatives
4	2.48	353.0870	$C_{16}H_{18}O_9$	3-O-Caffeoylquinic acid	Caffeoylquinic Acid Derivatives
5	3.46	387.1656	$C_{18}H_{28}O_9$	Jasmonic acid: 7-Epimer, 12-hydroxy, O-β-D-glucopyranoside	Jasmonic acid
6	3.79	563.1400	$C_{26}H_{28}O_{14}$	Apigenin 7-glycosides: 7-O-[β-D-Apiofuranosyl-(1 → 2)-β-D-glucopyranoside]	Flavonoid glycoside
7	4.03	577.1558	$C_{27}H_{30}O_{14}$	Apigenin 4′-7-diglycoside: 4-O-α-L-Rhamnopyranoside, 7-O-β-D-glucopyranoside	Flavonoid glycoside
8	4.21	515.1182	$C_{25}H_{24}O_{12}$	6-C- β-D-glucopuranosyl-4′,5,7-trihydroxyflavone:2″,6″-Di-Ac	Flavonoid glycoside
9	4.36	549.1965	$C_{27}H_{34}O_{12}$	2,7′-Cyclo-2′,9-epoxy-8,8′-lignan-3,3′,4,4′,5,5′,9′-heptol: (7′R,8S,8′S)-form, 3,3′,5,5′-Tetra-Me ether, 9′-O-β-D-xylopyranoside	Flavonoid glycoside
10	4.50	575.2704	$C_{27}H_{44}O_{13}$	3,11-Dihydroxy-3-eudesmen-2-one: 3,11-Di-O-β-D-glucopyranoside	Eudesmanegluscoside
11	4.76	563.2122	$C_{28}H_{36}O_{12}$	4,7′-Epoxy-3,8′-lign-7-ene-3′,4′,5,5′,9,9′-hexol: (7E,7′R,8′S)-form, 3′,4′,5,5′-Tetra-Me ether, 9-O-β-D-glucopyranoside	Neolignans glucoside
12	6.36	459.3838	$C_{30}H_{52}O_3$	3-Alkyl-5-methoxy-2-methyl-1,4-benzoquinones: 3-Docosyl-5-methoxy-2-methyl-1,4-benzoquinone	Quinones
13	6.71	555.2836	$C_{28}H_{44}O_{11}$	7(14)-Bisabolene-1,2,3,4,5,8,10,11-octol: (1α,2α,3β,4α,5α,6αH,8ξ,10ξ)-form, 11-Me ether, 2,8-diangeloyl, 5-Ac	Sesquitepenoid
14	7.08	459.3837	$C_{30}H_{52}O_3$	2,3,16-Friedelanetriol	Triterpene
15	7.42	521.3115	$C_{29}H_{46}O_8$	22,26-Epoxy-2,3,14,20,24,26-hexahydroxystigmast-7-en-6-one	Steroid (cyasterone)

R.T.: Retention time, $[M-H]^+$: Molecular ion, M.F: Molecular formula.

(2) *Antimalarial activity*

Herein, EA extract showed noteworthy ($p < 0.05$) antimalarial potential with an IC_{50} of 3.5 ± 0.07 and 9.02 ± 0.39 μg/ml, against D6 and W2, respectively (Fig. 4). Rest of the samples also manifested a moderately significant antimalarial potential. Minimum antimalarial potential was exhibited by DW extract. DMSO did not show any inhibition.

3.3.4. Cytotoxic potential of *A. brevifolia* extracts

(1) *Cytotoxicity against A. salina (Brine shrimps)*

All the tested manifested notable($p < 0.05$) shrimp's lethality potential (Table 6). EA extract was found to be highly potent with LD_{50} of 25 ± 1.9 μg/ml. It was followed by NH and M extracts. Minimum cytotoxic potential was exhibited by DW extract with LD_{50} 40.3 ± 3.7 μg/ml. Positive control used was doxorubicin, which demonstrated the LD_{50} 5.98 ± 0.2 μg/ml whereas DMSO did not reveal any toxicity.

(2) *Cytotoxicity against cancer cell lines*

Almost all the extracts demonstrated substantial ($p < 0.05$) cytotoxic potential against tested human cancer cell lines (Table 6). Among all the extracts, EA showed a comparatively significant ($p < 0.05$) potential, against all the cell lines except MCF-7. NH and M extracts were active against HepG2 and DU-145 cell lines (IC_{50} 19.6 ± 1.1; 19.0 ± 0.2 and 18.66 ± 2.9; 18.82 ± 0.4 μg/ml,

Table 4
Phytochemistry, antioxidant and *in vitro* anti-inflammatory potential of *A. brevifolia*extracts.

Samples	Phytochemical assays		Antioxidant assays						*In vitro* anti-inflammatory assay
	TPC	TFC	TAC	TRP	FRSA		β-carotene bleaching potential	Iron chelating potential	Nitric oxide scavenging potential
	µg GAE/mgE	**µg QE/mgE**	**µg AAE/mgE**	**µg AAE/ mgE**	**POI**	**IC_{50} (µg/ml)**	**IC_{50} (µg/ml)**	**IC_{50} (µg/ml)**	**IC_{50} (µg/ml)**
	400 µg/ml		**200 µg/ml**						
NH	1.42 ± 0.038^{d}	1.62 ± 0.02^{d}	14.2 ± 0.4^{d}	16.6 ± 0.6^{d}	1.15 ± 0.06^{d}	>200^{a}	>200^{a}	165.74 ± 2.76^{a}	>200^{a}
EA	4.2 ± 0.039^{c}	2.82 ± 0.296^{c}	19.72 ± 0.88^{c}	25.4 ± 1.0^{c}	12.28 ± 2.65^{c}	>200^{a}	>200^{a}	139.45 ± 0.97^{b}	161.07 ± 2.86^{b}
M	16.96 ± 0.12^{a}	10.30 ± 0.48^{a}	65.7 ± 0.4^{a}	112.3 ± 1.2^{a}	85.75 ± 0.38^{a}	21.15 ± 0.01^{b}	45.44 ± 1.23^{c}	28.21 ± 1.18^{d}	19.91 ± 2.03^{d}
DW	10.25 ± 0.28^{b}	7.26 ± 0.026^{b}	43.45 ± 0.42^{b}	78.9 ± 2.3^{b}	81.01 ± 0.18^{b}	21.68 ± 0.04^{b}	52.03 ± 2.56^{b}	45.33 ± 2.06^{c}	37.83 ± 1.99^{c}

Results presented are the mean ± SD of triplicate analysis. Means with different superscript (a–d) letters in the column are significantly ($p < 0.05$) different from one another. —: No activity detected, ***: Not evaluated, NH: n-hexane, EA: Ethyl acetate, M: Methanol, DW: Distilled water, POI: Percent of inhibition, TPC: Total phenolic content, TFC: Total flavonoid content, TAC: Total antioxidant capacity, TRP: Total reduction potential, FRSA: Free radical scavenging assay.

respectively). DW extract was found active against THP-1 cell line with an IC_{50} value of 18.6 ± 1.9 µg/ml.All the extracts were found most active against THP-1 cell line. The cytotoxic potential of *A. brevifolia*was evaluated for the first time. DMSOdid not exhibit cytotoxicity.

(3) *Cytotoxicity against isolated lymphocytes*

Cytotoxic potential of the extracts was also evaluated against isolated lymphocytes at similar concentration used for cytotoxicity assessment against cancer cell lines (Table 6). Data clearly indicates that none of the extracts exhibited toxicity against the isolated lymphocytes. Vincristine, showed significant cytotoxicity against the isolated cells with IC_{50} value of 6.7 ± 1.5 µg/ml.

3.3.5. Genotoxicity assays

(1) *Comet assay*

Maximum DNA damage was produced by cisplatin ($p < 0.05$). Herein, %DNA migration of 47.7 ± 1.4%, 50.8 ± 1.4%, 50.7 ± 1.7% and 45.9 ± 0.7 %of comet's tail was observed in case of HepG2, THP-1, HT-29 and DU-145 cell lines, respectively (Table 7). Extracts did not induce DNA damage, as %tail DNA ranges from 3.17 ± 0.1to 7.69 ± 0.2% in different cancer cell lines, exhibiting the safe behavior of *A. brevifolia.* Negative control also did not depict genotoxicity as 5.36 ± 0.1was the maximum %tail DNA observed in case of DMSO (Fig. 5).

(2) *Micronucleus assay*

Effects of four different extracts of *A. brevifolia* on %MN formation per 1000 BN cells and NDI values have been presented in Table 7. Cisplatin significantly ($p < 0.05$) increased the chromosomal damage in all the cell lines with minimum %MN formation observed in DU-145 cell lines (22.5 ± 2%). It is quite evident from the results that extracts did not induce any significant MN formation as compared to intact control. DMSO also did not induce any DNA damage. Maximum %MN formation, in case of DMSO (1.83 ± 0.2%) was observed in HepG2 cells. While measuring the second parameter which is NDI, CP alone insignificantly decreased NDI when compared to the untreated cells, i.e., 1.03 ± 0.1, 1.05 ± 0.2, 1.12 ± 0.1 and 1.01 ± 0.1 in HepG2, THP-1, HT-29 and DU-145 cell lines. The NDI was comparatively higher in extracts treated cells as compared to cells treated with positive control. Results clearly indicate that *A. brevifolia* extracts did not induce genotoxicity.

(3) *Chromosomal aberration assay*

Anticlastogenic effect of the extracts was observed through chromosomal aberration assay (Table 7). The number of aberrant metaphases (NAMP) observed in cisplatin treated cells were significantly ($p < 0.05$) higher than extracts treated cell lines. In case of HepG2 cells, maximum NAMP (38) was observed in cisplatin treated cells whereas within the extracts treatment it ranges from 1 to 3. DMSO did not induce any significant aberration as total 2 aberrations were observed. Similar was the case observed in other cell lines, i.e., THP-1, HT-29 and DU-145 where total NAMP,within the extracts treated groups, ranges from 1 to 3, 1 to 2 and 1 to 3, respectively. A noteworthy difference in the total number of chromosomal aberrations (TNCA), in comparison to cisplatin, was observed. TNCA was found to be maximum in CP treated cells, i.e., 57, 58, 59 and 52 in HepG2, THP-1, HT-29 and DU-145 cell lines, respectively. Maximum TNCA in NH treated cells was 2, which was observed in HepG2 cell lines whereas it was 3 (HepG2 cell lines) in case of EA extract, 2 (all the cell lines tested) in case of M extract and 2 (HepG2 and HT-29 cell lines) in case of DW extract. A significant reduction in the key cytogenetic parameters was also revealed.

3.3.6. Anti-inflammatory assays

(1) *In vitro nitric oxide scavenging assay*

A significant NO scavenging activity was depicted by all the extracts (Table 4). Maximum scavenging potential ($p < 0.05$) was shown by M extract (IC_{50} 19.91 ± 2.03 µg/ml) followed by DW and EA extracts, respectively. NH exhibited the least scavenging with IC_{50}>200 µg/ml. Ascorbic acid (positive control) exhibited an IC_{50} of 5.47 ± 0.38 µg/ml whereas DMSO did not show any activity.

(2) *In vivo carageenan induced paw edema inhibition assay*

Mostly testedexhibited highest effects in 4th h of treatment (Fig. 6). Among all extracts, M extract showed significant ($p < 0.05$) inhibition of edema at high dose of 300 mg/kg BW, i.e., 30.1 ± 2.4, 50 ± 2.1, 65.7 ± 2.12 and 77.22 ± 1.9% in comparison to ibuprofen (standard drug used). Ibuprofen exhibited an edema inhibition of 18.8 ± 0.93, 49.59 ± 1.8, 77.67 ± 2.9 and 90.52 ± 2.9% at 1st, 2nd, 3rd and 4th h, respectively. Inhibition potential of edema decreased in the following trend among the extracts; MH > ML > DWH > DWL > EAH > EAL > NHH > NHL.

Table 5
Antibacterial and antifungal activities of *A.brevifolia* extracts.

Samples	Antibacterial potential									Antifungal potential					
	Diameter of zone of inhibition (ZOI: mm) & MIC (µg/ml)														
	Strains	ZOI	MIC	Strains	ZOI	MIC	Strains	ZOI	MIC	Strains	ZOI	MIC	Strains		
NH	*K. pneumoniae*	17 ± 0.2^{c}	200^{a}	*B. subtilis*	16 ± 0.3^{c}	66.66^{a}	Methicillin Resistant	17 ± 0.56^{c}	66.66^{a}	*Mucor* Spp.	–	***	*A. flavus*	–	***
EA		18 ± 0.4^{b}	200^{a}		20 ± 0.4^{b}	22.22^{b}	*S. aureus*	22 ± 0.34^{a}	22.22^{b}		–	***		–	***
M		13 ± 0.2^{d}	200^{a}		9 ± 0.87^{e}	–		19 ± 0.52^{b}	66.66^{a}		–	***		17 ± 0.98^{b}	66.66^{a}
DW		11 ± 0.3^{e}	–		10 ± 0.5^{d}	–		9 ± 0.23^{d}	–		–	***		–	***
Cefixime		20 ± 0.2^{a}	1.11^{b}		***	***		***	***		***	***		***	***
Roxithromycin		***	***		22 ± 0.6^{a}	1.11^{c}		–	–		***	***		***	***
Clotrimazole		***	***		***	***		***	***		36 ± 0.75^{a}	2.5^{a}		34 ± 1.03^{a}	10^{b}
DMSO		–	–		–	–		–	–		–	–		–	–
NH	*S. aureus*	20 ± 0.3^{b}	22.22^{b}	*P. aeruginosa*	18 ± 0.3^{c}	66.66^{b}	Resistant *E. coli*	17 ± 0.12^{a}	66.66^{b}	*F. solani*	–	***	*A. fumigatus*	–	***
EA		19 ± 0.5^{c}	66.66^{a}		21 ± 0.3^{b}	22.22^{c}		14 ± 0.15^{c}	200^{a}		19 ± 0.07^{b}	66.66^{a}		20 ± 0.3^{b}	22.22^{b}
M		7 ± 0.21^{d}	–		16 ± 0.2^{d}	66.66^{b}		15 ± 0.63^{b}	200^{a}		–	***		19 ± 0.9^{c}	66.66^{a}
DW		7 ± 0.5^{d}	–		12 ± 0.9^{e}	200^{a}		10 ± 0.42^{e}	–		10 ± 0.67^{c}	***		–	***
Cefixime		***	***		22 ± 0.8^{a}	1.11^{d}		11 ± 1.5^{d}	***		***	***		***	***
Roxithromycin		23 ± 0.5^{a}	1.11^{c}		***	***		***	***		***	***		***	***
Clotrimazole		***	***		***	***		***	***		30 ±.19^{a}	5^{b}		36 ± 0.9^{a}	5^{c}
DMSO		–	–		–	–		–	–		–	–		–	–
NH	*E. coli*	21 ± 0.2^{c}	22.22^{b}	Resistant	20 ± 0.5^{a}	22.22^{b}	Resistant	11 ± 0.44^{c}	–	*A. niger*	7 ± 0.31^{c}	***			
EA		20 ± 0.3^{d}	22.22^{b}	*P. aeruginosa*	19 ± 0.2^{b}	66.66^{a}	*S. hemolyticus*	19 ± 0.83^{a}	66.66^{b}		–	***			
M		25 ± 0.3^{b}	22.22^{b}		19 ± 0.7^{b}	66.66^{a}		12 ± 0.32^{b}	200^{a}		–	***			
DW		15 ± 0.7^{e}	66.66^{a}		10 ± 0.5^{c}	–		9 ± 0.29^{d}	–		8 ± 0.32^{b}	***			
Cefixime		26 ± 3.5^{a}	1.11^{c}		–	–		***	***		***	***			
Roxithromycin		***	***		***	***		–	–		***	***			
Clotrimazole		***	***		***	***		***	***		30 ± 0.37^{a}	5^{a}			
DMSO		–	–		–	–		–	–		–	–			

Values presented are the mean ± SD of triplicate analysis. Means with different superscript (a–e) letters in the row are significantly ($p < 0.05$) different from one another. —: No activity detected, ***: Not evaluated, NH: n-hexane, EA: Ethyl acetate, M: Methanol, DW: Distilled water, DMSO: Dimethyl sulfoxide.

Table 6
Cytotoxic potential of *A. brevifolia* extracts.

Samples	Cytotoxicity against brine shrimps (*A.salina*), isolated lymphocytes& cancer cell lines															
	LD_{50} & IC_{50} (µg/ml); Percent of inhibition (%In)															
	A.salina	Lymphocytes		A2780		HepG2		THP-1		HT-29		DU-145		MCF-7		
	LD_{50}	%In	IC_{50}	%In	IC_{50}	%In	IC_{50}	%In	IC_{50}	%In	IC_{50}	%In	IC_{50}	%In	IC_{50}	
NH	27.7 ± 0.9^{c}	5.4 ± 1.6^{c}	>20^{a}	41.2 ± 1.4^{c}	—	51.1 ± 0.7^{d}	19.6 ± 1.1^{a}	69.1 ± 0.7^{c}	14.5 ± 0.2^{c}	53.3 ± 1.9^{c}	18.8 ± 1.4^{a}	53.6 ± 3.5^{c}	18.7 ± 2.9a	27.2 ± 5.0^{d}	—	
EA	25 ± 1.9^{d}	6.3 ± 1.3^{b}	>20^{a}	55.4 ± 1.6^{b}	18.1 ± 0.9^{a}	69.5 ± 0.4^{b}	14.4 ± 0.2^{b}	71.1 ± 1.7^{b}	14.1 ± 2.9^{c}	62.2 ± 3.3^{b}	16.2 ± 0.9^{b}	64.7 ± 2.3^{b}	15.6 ± 0.2b	34.7 ± 8.2^{b}	—	
M	35.4 ± 0.4^{b}	2.7 ± 0.8^{e}	>20^{a}	36.5 ± 1.5^{d}	—	52.6 ± 0.2^{c}	19.0 ± 0.2^{a}	66.6 ± 0.2^{d}	15.1 ± 2.1^{b}	43.8 ± 6.3^{d}	—	53.1 ± 1.9^{c}	18.8 ± 0.4a	19.8 ± 3.9^{e}	—	
DW	40.3 ± 3.7^{a}	3.2 ± 0.6^{d}	>20^{a}	31.7 ± 1.2^{e}	—	36.8 ± 0.3^{e}	—	53.8 ± 0.3^{e}	18.6 ± 1.9^{a}	33.5 ± 5.2^{e}	—	21.7 ± 3.8^{d}	—	29.3 ± 14.1^{c}	—	
Positive and negative standards																
DR	5.98 ± 0.2^{e}	***		***		98.9 ± 0.2^{a}	1.71 ± 0.2^{c}	***		***		***		98.6 ± 0.1^{a}	1.03 ± 0.4^{a}	
VC		77.4 ± 3^{a}	6.7 ± 1.5^{b}	***		***		99.2 ± 0.3^{a}	0.76 ± 0.2^{e}	***		***		***		
CP	***	***		***		***		***		***		***		***		
5-FU	***	***		***		***		99.2 ± 0.9^{a}	2.01 ± 0.1^{d}	98.2 ± 1.5^{a}	2.91 ± 0.1^{c}	***	0.05 ± 0.5^{c}	***		
DMSO	—	—	—	—	—	—	—	—	—	—	—	—	—	—	—	

Results are presented as mean ± SD (n = 3). Means with different superscript (a–e) letters, are significantly ($p < 0.05$) different from one another. —: No activity detected, ***: Not evaluated, NH: n-hexane, EA: Ethyl acetate, M: Methanol, DW: Distilled water, CP: Cisplatin, DR: Doxorubicin, VC: Vincristine, 5-FU: 5-Fluoruracil, DMSO: Dimethly sulfoxide.

The NH extract exhibited least inhibition activity at both high and low doses. Vehicle control did not exhibited any activity.

(3) *In vivo croton oil induced anal edema inhibition assay*

Results showed that polar extracts demonstrated a significant ($p < 0.05$) activity in comparison to nonpolar extracts (Fig. 6). Highest anti-inflammatory potential was revealed by DW extract (74. 44 ± 0.96%) as compared to ibuprofen (86.85 ± 2.4%). It was followed by M (57.22 ± 2.5%), EA (52.04 ± 0.71%) and NH (33.33 ± 1. 01%) extracts. Vehicle control did not induce any activity.

3.3.7. Enzyme inhibition assays

(1) *α-amylase inhibition assay*

Significant ($p < 0.05$) carbohydrate-metabolizing enzyme inhibition was exhibited by DW and M extractswith IC_{50} values of 89.7 ± 1.08 and 105.74 ± 1.43 µg/ml, respectively (Fig. 7). Rest, EA and NH extracts depicted amoderate enzyme inhibition, i.e., 42.21 ± 0.987% and 33.91 ± 0.987%, respectively. Acarbose, the positive control used, exhibited an IC_{50} value of 33.73 ± 0.12 µg/ml.

(2) *α-glucosidase inhibition assay*

Inhibition of carbohydrate-metabolizing enzymes was further investigated by α-glucosidase inhibition assay (Fig. 7). The DW extract showed notable ($p < 0.05$) α-glucosidase inhibition (IC_{50} value of 98.14 ± 0.47 µg/ml). Minimal enzyme inhibition was exhibited by M, NH and EA extracts, respectively.

4. Discussion

Artemisia brevifolia is one of the pharmacologically active plants of genus *Artemisia* that has been used in traditional medicine to treat various ailments. Despite its effectiveness, scientific evidence proving its medicinal properties, is insufficient. Thus, in the current study, we evaluated pharmacological potential of *Artemisia brevifolia* via a battery of assays. Initially, different extracts were prepared by successive extraction using solvents of variable polarity. Extraction is considered a potential limiting step while preparing plants' samples for screening of the desired bioactivities (Ahmed et al., 2017). Its efficiency is usually affected by the nature of the solvent, solvent-to-solid ratio, particle size of grounded plant material, extraction duration and temperature. Extraction efficiency can be augmented by ultrasonic-assisted maceration (UAM) that accelerates solvent diffusion and dissolution of the solute. Furthermore, a significant ($p < 0.05$) increment in the extraction yield has been observed when solvents of different polarity are used, from non-polar to polar edge (Zahra et al., 2017). Both UAM and variable solvent polarity aided in better extract recovery in our study providing a range of phytoconstituents.

Next, phytoconstituents particularly polyphenolic compounds, artemisinin and its derivatives were quantified in extracts. Results clearly indicate that polar solvents, i.e., M and DW, exhibited better yield of total phenolic and flavonoid compounds, thus signifying the role of extraction solvents' polarity (Table 4). These findings are in agreement with previous studies where significant amount of phenols were quantified in methanol extracts of *A. campestris* (Mourad et al., 2018). Iqbal et al.(2012) also reported polar solvents as better extraction media for flavonoids. The conjugation of hydroxyl groups with glycosidic part might be responsible for better solubility in polar solvents. Moreover, it is predicted for the plant to have a good pharmacological profile due to the presence of these polyphenols. Literature has shown that phenolic and flavonoid compounds, owning to the presence of ketonic, hydroxyl/methoxy groups and benzo-y-pyrone ring, impart credible antioxidant properties either by free radical scavenging, singlet oxygen

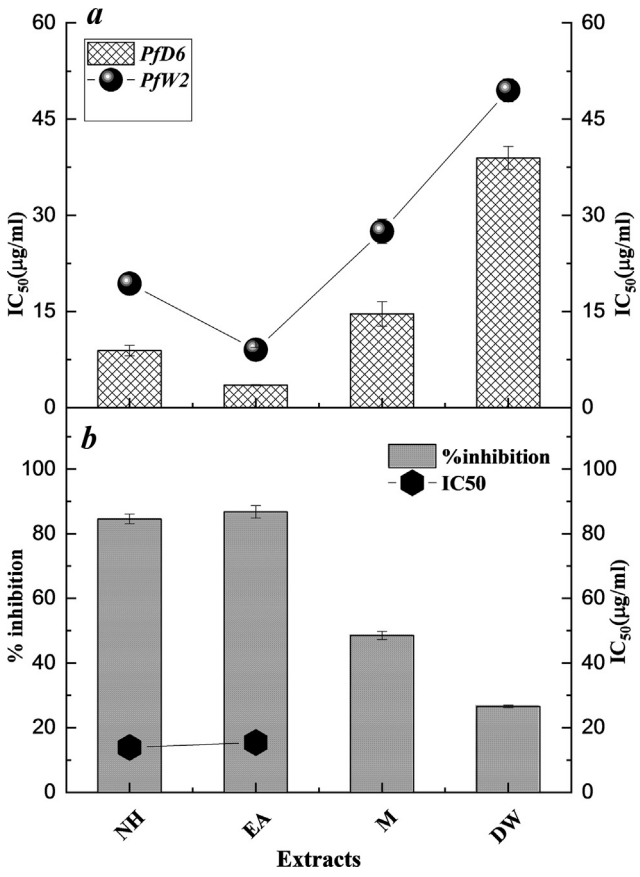

Fig. 4. Antimalarial (a) and antileishmanial (b) potentials of *A. brevifolia* extracts. Values are presented as mean ± SD from triplicate investigation. NH: n-Hexane, EA: Ethyl acetate, M: Methanol, DW: Distilled water.

quenching, metal ion chelation, hydrogen donation or inhibition of lipid peroxidation. These exhibit diverse pharmacological properties, e.g., anti-inflammatory, antiulcer, antioxidant, antispasmodic, antitumor, and antidepressant activities (Fatima et al., 2015, Nasir et al., 2017). Flavonoids are the major phytonutrients of species belonging to genus *Artemisia*, i.e., *A. vulgaris, A. absinthium, A. campestris, A. spicigera and A. splendens* (Iqbal et al., 2012).

Chromatographic finger printing through RP-HPLC-DAD analysis evinced significant amounts of emodin, luteolin, vanillic acid, syringic acid in EA extract. These compounds have been used in traditional Chinese medicine for their respective immunostimulant (Zahra et al., 2017), enzyme inhibitory, genoprotective, antithrombotic (Fatima et al., 2015) and antiendotoxic (Srinivasulu et al., 2018) properties. Gallic acid, detected in M and DW extracts, has well reputed antioxidant, immuno-modulatory and antileishmanial potential (Fatima et al., 2015). Furthermore, artemisinin, dihydroartemisinin, artesunate and artemether were found in NH, EA and M extracts of *A. brevifolia*. Maximum amount of these antimalarial compounds was quantified in EA extract. The δ-lactone ring and endoperoxide bridge in the structure of these compounds make them weakly polar (Liu et al., 2009). On the basis of "like dissolve like" ethyl acetate (weakly polar solvents) extracted more amounts are compared to other solvents. Thus, here we present EA extract of *A. brevifolia,* an ample source of artemisinin and its derivatives.

HRMS analysis of *A. brevifolia* extracts evinced 40 chemical compounds in M and DW extracts. Polyphenolic compounds, sesquiterpenoids and lignin glycosides served as major phytonutrients of M extract whereas former class was dominant in DW extract. Results endorse better solubility of both of these chemical classes in polar solvents. These compounds have reported anti-osteoporotic, antidiabetic, hepatoprotective (Nasir et al., 2020), antimalarial, antileishmanial (Rohmer 1999) and anticancer potential. Lignin glycosides were found active against different human breast cancer cell lines (Bt549, MCF7 and MDA-MB-231) (Baek et al., 2018). A straight chain alkane, heneicosane derivative, was also detected in DW extract. This compound is reported to attract mosquitoes in lower concentration whereas at higher concentration they are repelled instead (Seenivasagan et al., 2009). Significant ($p < 0.05$) pharmacological potential of *A. brevifolia* extracts observed in the current study might be attributed to the presence of these compounds.

The pharmacological profile of *A. brevifolia* was established by antioxidant, anti-inflammatory, antileishmanial, antimalarial, antibacterial, antifungal and cytotoxic activities. Yin-yang, a complex relational concept in traditional Chinese medicine, expounds the importance of balance between oxidants and antioxidants. Oxidants, generated as byproducts at physiological concentrations, are required for numerous cellular functions. However, disproportionate production induces oxidative stress, which impairs the integrity of vital biomolecules and triggers numerous ailments (Kazmi et al., 2018). Supplementing with exogenous natural antioxidants is plausible (Majid et al., 2018). Currently,M extract of *A. brevifolia* depicted maximum FRSA. M and DW extracts demonstrated highest antioxidant potential while evaluated through a battery of antioxidant assays. Results are in accordance with previous studies where methanol extract of *A. absinthium* (EREL et al., 2012), *A. annua* leaves (Iqbal et al., 2012) and polar extracts of *A. campestris* (Akrout et al., 2011) showed significant total antioxidant capacity, free radical scavenging and β-carotene scavenging potential. Currently, a number of polyphenolic compounds have been detected in *A. brevifolia* extracts. Significant ($p < 0.05$) antioxidant assertiveness might be accredited to the presence of these compounds. These compoundsexert the antioxidant effects by virtue of the hydroxyl groups (Kazmi et al., 2018). In addition, total reduction potential of *A. brevifolia*extracts might be attributed to the presence of artemisinin, which is known to reduce ferric ions to ferrous (Sibmooh et al., 2001).

Iron chelating assay involves the sample's ability to chelate with iron (II), thus hampering the iron-ferrozine complex formation and lowering color intensity of the solutions. Our findings are in consensus with that of Majid et al. (2015)as M and DW extracts exhibited significant ($p < 0.05$) iron chelation potential in comparison to Catechin. In contrast to other antioxidant assays, herein, NH and EA extracts also gave moderately significant ($p < 0.05$) results. This potential might be associated to the presence of artemisinin and its analogues, as they chelate with iron to exert their antimalarial effect (O'neill et al., 2010).

Subsequently, anti-infective activity of *A. brevifolia* extracts was determined against bacterial, fundal, malarial and leishmanial strains. Emergence of multidrug-resistant phenotypes of several pathogenic bacterial strains is a major health problem in the treatment of infections. Likewise, complications including hypersensitivity reactions and myelosuppression make it difficult to use certain antibiotics (Zahra et al., 2017). Current study presents *A. brevifolia* EA and NH extracts as possible source of antibacterial agents since they demonstrated significant ($p < 0.05$) inhibition of tested bacterial strains including *P. aeruginosa* and MRSA. Polyphenolic compounds inhibit microbial enzymes either by reacting with sulfhydryl groups or by interacting with the proteins leading to microbial growth inhibition (Fatima et al., 2015). Moreover, sesquiterpenes are known to have strong antibacterial profile (Rohmer, 1999). Therefore, espied antimicrobial potential of the extracts can be ascribed to the presence of detected compounds (Rohmer, 1999).Compounds isolated from these extracts are

Table 7
Effect of *A.brevifolia* extracts on DNA integrity of cancer cell lines.

Cell lines employed		Comet assay						Micronucleus assay		Chromosomal assay									
											No. of chromosomal aberrations								
											Chromatid		Isochromatid		Exchange				
	Samples	CL (μm)	HL (μm)	TL (μm)	%DIH	%DIT	TM	%MN	NDI	NAMP	g	b/f	g	b/f	dic	qr	Tr	DM	TNCA
HepG2	NH	55 ± 0.5^{d}	52 ± 0.4^{d}	3 ± 0.8^{c}	94.55 ± 0.8^{d}	5.45 ± 0.1^{c}	0.99 ± 0.1^{b}	0.5 ± 0.07^{f}	1.81 ± 0.1^{c}	2^{c}	1^{b}	2^{b}	–	–	–	–	–	–	2^{d}
	EA	52 ± 1.8^{e}	50 ± 1.5^{e}	2 ± 1.3^{d}	96.15 ± 0.2^{b}	3.85 ± 0.2^{e}	0.57 ± 0.1^{d}	0.57 ± 0.2^{e}	1.86 ± 0.3^{a}	2^{c}	–	1^{c}	–	1^{b}	–	–	1^{b}	–	3^{c}
	M	62 ± 0.5^{b}	59 ± 1.6^{b}	3 ± 1.8^{c}	95.16 ± 0.4^{c}	4.84 ± 0.1^{d}	0.63 ± 0.1^{c}	0.46 ± 0.1 ^{g}	1.78 ± 0.2^{d}	3^{b}	–	1^{c}	–	1^{b}	–	–	–	–	2^{d}
	DW	52 ± 1.8^{e}	47 ± 1.3^{f}	5 ± 0.9^{b}	92.31 ± 0.5^{e}	7.69 ± 0.2^{b}	0.1 ± 0.01^{f}	0.61 ± 0.1^{c}	1.69 ± 0.2^{f}	1^{d}	–	1^{c}	–	1^{b}	–	–	–	–	2^{d}
	IC	61 ± 0.9^{c}	58 ± 0.5^{c}	3 ± 0.1^{c}	95.08 ± 0.2^{c}	4.92 ± 0.1^{d}	0.2 ± 0.03^{e}	0.59 ± 0.2^{d}	1.73 ± 0.2^{e}	3^{b}	1^{b}	2^{b}	–	1^{b}	1^{b}	–	–	–	4^{b}
	DMSO	62 ± 1.5^{b}	61 ± 1.4^{a}	1 ± 0.1^{e}	98.39 ± 0.9^{a}	1.61 ± 0.1^{f}	0.1 ± 0.02^{f}	0.63 ± 0.1^{b}	1.83 ± 0.2^{b}	2^{c}	–	1^{c}	1^{a}	1^{b}	–	–	–	–	2^{d}
	CP	67 ± 1.3^{a}	35 ± 2.5 ^{g}	32 ± 1^{a}	52.23 ± 1.4^{f}	47.7 ± 1.4^{a}	10.2 ± 0.2^{a}	25.4 ± 1.2^{a}	1.03 ± 0.1 ^{g}	38^{a}	2^{a}	36^{a}	–	8^{a}	6^{a}	4^{a}	3^{a}	–	57^{a}
THP-1	NH	52 ± 1.5 ^{g}	50 ± 1.9^{e}	2 ± 0.4^{d}	96.15 ± 0.2^{b}	3.85 ± 0.2^{e}	0.24 ± 0.1 ^{g}	0.8 ± 0.1^{b}	1.77 ± 0.3^{c}	1^{d}	–	–	–	–	–	1^{b}	–	–	1^{e}
	EA	64 ± 1.5^{b}	61 ± 1.9^{b}	3 ± 0.4^{c}	95.31 ± 1.9^{c}	4.69 ± 0.2^{d}	0.22 ± 0.1^{c}	0.73 ± 0.2^{c}	1.81 ± 0.1^{b}	1^{d}	–	–	–	1^{b}	–	–	–	–	1^{e}
	M	53 ± 1.2^{f}	49 ± 2.0^{f}	4 ± 0.9^{b}	92.45 ± 2.4^{e}	7.55 ± 0.1^{b}	0.6 ± 0.3^{d}	0.60 ± 0.1^{d}	1.73 ± 0.3^{d}	3^{b}	–	1^{c}	–	1^{b}	–	–	–	–	2^{d}
	DW	58 ± 0.8^{e}	55 ± 1.1^{d}	3 ± 0.4^{c}	94.83 ± 0.8^{d}	5.17 ± 0.2^{c}	0.76 ± 0.2^{e}	0.77 ± 0.3^{c}	1.72 ± 0.2^{e}	1^{d}	–	1^{c}	–	–	–	–	–	–	1^{e}
	IC	62 ± 3.4^{d}	59 ± 2.4^{c}	3 ± 0.3^{c}	95.16 ± 1.4^{c}	4.84 ± 0.2^{d}	1.4 ± 0.01^{b}	0.49 ± 0.1^{e}	1.85 ± 0.1^{a}	2^{c}	–	1^{c}	–	1^{b}	1^{b}	1^{b}	1^{b}	–	5^{b}
	DMSO	67 ± 0.4^{a}	65 ± 1.4^{a}	2 ± 1.9^{d}	97.01 ± 0.2^{a}	2.99 ± 0.1^{f}	0.52 ± 0.1^{f}	0.81 ± 0.1^{b}	1.73 ± 0.3^{d}	3^{b}	1^{b}	2^{b}	–	1^{b}	1^{b}	–	–	–	4^{c}
	CP	63 ± 1.4^{c}	31 ± 1.7 ^{g}	32 ± 2^{a}	49.20 ± 2.2^{f}	50.8 ± 1.4^{a}	11.4 ± 0.5^{a}	29.6 ± 4.9^{a}	1.05 ± 0.2^{f}	33^{a}	2^{a}	26^{a}	–	9^{a}	8^{a}	10^{a}	5^{a}	–	58^{a}
HT-29	NH	51 ± 0.3^{f}	48 ± 3.1^{e}	3 ± 0.8^{b}	94.12 ± 1.9^{c}	5.88 ± 0.1^{b}	0.89 ± 0.3^{b}	0.87 ± 0.1^{b}	1.91 ± 0.4^{a}	1^{d}	1^{b}	–	–	1^{b}	–	–	–	–	1^{d}
	EA	56 ± 2.5^{d}	53 ± 1.4^{c}	3 ± 0.9^{b}	94.64 ± 2.6^{c}	5.36 ± 0.1^{b}	0.99 ± 0.2^{d}	0.65 ± 0.3^{d}	1.71 ± 0.1^{f}	2^{c}	1^{b}	1^{c}	–	1^{b}	–	–	–	–	2^{c}
	M	63 ± 0.2^{c}	61 ± 2.3^{b}	2 ± 0.3^{c}	96.83 ± 1.0^{a}	3.17 ± 0.1^{d}	0.82 ± 0.1^{f}	0.42 ± 0.1 ^{g}	1.75 ± 0.2^{e}	2^{c}	–	1^{c}	–	1^{b}	–	–	–	–	2^{c}
	DW	66 ± 3.2^{b}	63 ± 2.9^{a}	3 ± 0.2^{b}	95.45 ± 1.8^{b}	4.55 ± 0.2^{c}	0.64 ± 0.3^{c}	0.67 ± 0.2^{c}	1.86 ± 0.3^{b}	1^{d}	–	1^{c}	–	1^{b}	–	–	–	–	2^{c}
	IC	56 ± 2.1^{d}	53 ± 1.5^{c}	3 ± 0.1^{b}	94.64 ± 0.2^{c}	5.36 ± 0.1^{b}	0.92 ± 0.2^{e}	0.53 ± 0.1^{e}	1.82 ± 0.2^{c}	3^{b}	1^{b}	2^{b}	–	1^{b}	–	–	–	–	3^{b}
	DMSO	54 ± 1.5^{e}	52 ± 1.6^{d}	2 ± 0.8^{c}	96.30 ± 0.4^{a}	3.70 ± 0.1^{d}	0.61 ± 0.1 ^{g}	0.49 ± 0.1^{f}	1.78 ± 0.2^{d}	2^{c}	–	1^{c}	–	1^{b}	–	–	1^{b}	–	3^{b}
	CP	69 ± 1.0^{a}	34 ± 0.4^{f}	35 ± 1^{a}	49.27 ± 1.5^{d}	50.7 ± 1.7^{a}	11.2 ± 0.5^{a}	35.1 ± 4.5^{a}	1.12 ± 0.1 ^{g}	40^{a}	3^{a}	36^{a}	1^{a}	8^{a}	5^{a}	5^{a}	4^{a}	1^{a}	59^{a}
DU-145	NH	61 ± 2.3^{b}	57 ± 0.9^{b}	4 ± 1.2^{b}	93.44 ± 0.7^{c}	6.56 ± 0.2^{c}	0.39 ± 0.3^{b}	0.58 ± 0.2^{c}	1.69 ± 0.2^{f}	1^{d}	1^{b}	–	–	–	1^{b}	–	–	–	1^{d}
	EA	56 ± 0.5^{d}	52 ± 2.8^{e}	4 ± 0.2^{c}	92.86 ± 2.1^{d}	7.14 ± 0.1^{b}	0.92 ± 0.2^{c}	0.43 ± 0.1 ^{g}	1.72 ± 0.2^{e}	3^{b}	1^{b}	1^{c}	–	1^{b}	–	–	–	–	2^{c}
	M	66 ± 1.7^{a}	63 ± 2.2^{a}	3 ± 0.9^{b}	95.45 ± 0.4^{a}	4.55 ± 0.1^{e}	0.65 ± 0.1^{f}	0.46 ± 0.1^{f}	1.84 ± 0.4^{a}	2^{c}	–	1^{c}	–	1^{b}	–	–	–	–	2^{c}
	DW	59 ± 2.1^{c}	56 ± 1.3^{c}	3 ± 0.3^{c}	94.92 ± 0.8^{b}	5.08 ± 0.2^{d}	0.74 ± 0.2^{d}	0.47 ± 0.2^{e}	1.76 ± 0.1^{d}	1^{d}	1^{b}	–	–	1^{b}	–	–	–	–	1^{d}
	IC	56 ± 1.1^{d}	52 ± 3.3^{e}	4 ± 0.2^{b}	92.86 ± 2.6^{d}	7.14 ± 0.1^{b}	1.29 ± 0.2^{c}	0.66 ± 0.1^{b}	1.82 ± 0.2^{b}	2^{c}	–	1^{c}	–	1^{b}	–	–	1^{b}	–	3^{b}
	DMSO	56 ± 0.8^{d}	53 ± 1.5^{d}	3 ± 0.3^{c}	94.64 ± 0.2^{b}	5.36 ± 0.1^{d}	0.70 ± 0.1^{e}	0.56 ± 0.2^{d}	1.77 ± 0.2^{c}	3^{b}	1^{b}	2^{b}	–	1^{b}	–	–	–	–	3^{b}
	CP	61 ± 0.9^{b}	33 ± 3.2^{f}	28 ± 3^{a}	54.10 ± 2.8^{e}	45.9 ± 0.7^{a}	10.9 ± 0.3^{a}	22.5 ± 2^{a}	1.01 ± 0.1 ^{g}	35^{a}	2^{a}	32^{a}	1^{a}	8^{a}	5^{a}	2^{a}	4^{a}	1^{a}	52^{a}

Results are presented as mean ± SD. Means with different superscript (a–g) letters, are significantly ($p < 0.05$) different from one another. CL: Comet length, HL: Head length, TL: Tail length, %DIH: Percent of DNA in head, %DIT: Percent of DNA in tail, TM: Tail moment, %MN: Percent of micronuclei/Binucleated cells counted, NDI: Nuclear division index, NAMP: No. of aberrant metaphases, g: Gap, b/f: Break/fragment, dic: Dicentric, qr: Quadriradial, tr: Triradial, dmin: Double minute, TNCA: Total number of chromosomal aberrations, NH: n-hexane, EA: Ethyl acetate, M: Methanol, DW: Distilled water, IC: intact control, CP: Cisplatin, DMSO: Dimethyl sulfoxide.

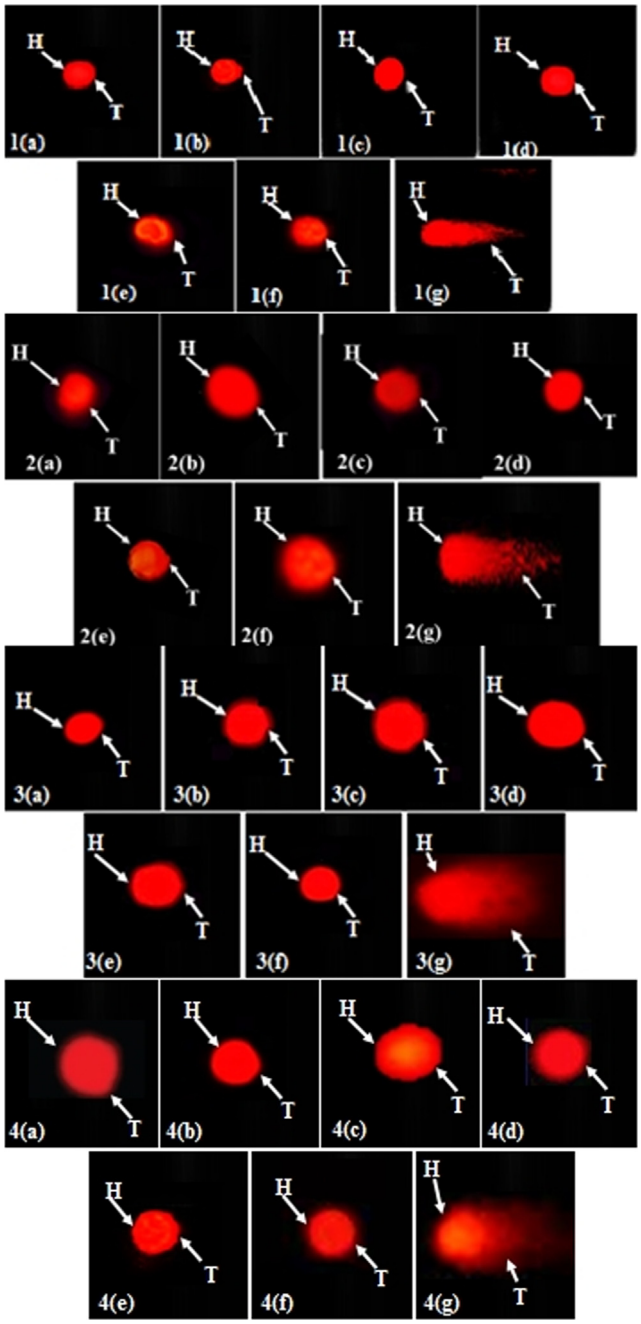

Fig. 5. Fluorescence micrograph for comet assay presenting the effects of *A. brevifolia* extracts on DNA of cancer cells. H: Comet's head, T: Comet's tail. 1: Hep G2 cell line, 2:THP-1 cell line, 3: HT-29 cell line, 4: DU-145 cell lines, a: NH, b: EA, c: M, d: DW extracts of *A. brevifolia*, e: intact control, f: Dimethyl sulfoxide, g: Cisplatin. NH: n-Hexane, EA: Ethyl acetate, M: Methanol, DW: Distilled water.

planned to be tested against resistant-strains. Those may become beneficial to prevent or treat MRSA induced endocarditis and toxic shock syndrome and *P. aeruginosa* induced sepsis (Parameswari et al., 2019), depending on the outcome of future studies.

A. brevifolia extracts manifested moderate significant ($p < 0.05$) activity against fungal strains. M extract demonstrated significant activity against *A. fumigatus* followed by EA extract, which was found active against *A. fumigatus* and *F. solani*. A number ofplants' secondary metabolites including terpenes, phenolics, phenolic glycosides, glucosinolates and flavonoids are known to exhibit antifungal potential (Rohmer 1999, Nasir et al., 2017). EA and M extracts of *A. brevifolia*, were found rich in sesquiterpenes and polyphenolic compounds, thatmight be responsible for their antifungal potential.

Another aspect of the study was to find an alternative source of antimalarial artemisinin. Malaria is among the top public health challenges that caused 5 million cases in WHO Eastern Mediterranean Regionin 2019 (Organization 2016). It is a common concern in Pakistan during every rainy season where emergence of drug resistant *Plasmodium falciparum* poses great threat. Since, *A. annua,* a major source of artemisinin, shares the same family with *A. brevifolia*; therefore, extracts of the selected plant were tested against both chloroquine sensitive (D6) and resistant strains (W2) of *P. falciparum* through flow cytometry. Flow cytometry is superior to other conventional method in analyzing malarial infection associated blood parasitemia. Basically, red blood cells (RBCs) primarily lack DNA. In case of infection, parasite metabolizes hydroethine into ethidium, a nucleic acid-binding fluorochrome. Therefore, counting the number of positively stained RBCs and comparing the ratio to the total number of RBCs represent blood parasitemia(Kaou et al., 2008). All the extracts of *A. brevifolia* have manifested a significant ($p < 0.05$) antimalarial potential with EA extract exhibiting the maximum. HPLC analysis of NH, EA and M extracts has confirmed the presence of artemisinin and its derivatives. These drugs usually act by endoperoxide moiety, which cleaves and generate free radicals ultimately killing the parasite by alkylation and inhibiting protein or nucleic acid synthesis (O'neill et al., 2010). Significant ($p < 0.05$) antimalarial potential of *A. brevifolia* extracts might be accredited to the presence of artemisinin and its derivatives. A number of polyphenolic compounds have also been detected through HPLC and HRMS studies. Antioxidant potential of these compounds can inhibit hemozoin formation letting heme free, which is very toxic for the malarial parasite (Abu-Lafi et al., 2020). Their presence also hinders the development of parasite resistance.

Next, effectiveness of extracts against leishmania was tested. Leishmaniasis, a neglected vector transmitted disease, has 1–1.5 million incidences of cutaneous while 0.5 million incidences of visceral leishmaniasis annually. Variable effectiveness, unacceptable side effects and emerging resistance against available drugs make them substandard (Waseem et al., 2017). Plant-derived products have gained eminent ground in search for better, effective and preferably non-toxic leishmanicidal compounds. A number of plant secondary metabolites including luteolin, vanillic acid, quassin, berberine and artemisinin have established antileishmanial profile (Ahmed et al., 2017). The presence of these compounds in *A. brevifolia* justifies its evaluation for antileishmanial potential.

Maximum antileishmanial potential was demonstrated by NH and EA extracts, which were found rich in sesquiterpenes and polyphenolics. Cytotoxicity of artemisinin in leishmanial promastigotes is mediated by a series of events, which are initiated by the cleavage of its endoperoxide bridge. This leads to prodigal ROS generation with concomitant non-protein thiols diminution and alteration of the mitochondrial membrane potential. Leishmanial parasite is more prone to oxidative stress as it cannot express catalase or peroxidase, the major H_2O_2 metabolizing enzymes. Moreover, a sole mitochondrion serves as the putative 'powerhouse' of the parasite. Therefore, modulation of the mitochondrial *trans*-membrane potential or inhibition of its respiratory complex, render it more vulnerable to plant-derived antileishmanial agents. All of these events culminated in a caspase-independent death, which mimics apoptosis (De Sarkar et al., 2019). Studies have shown that Totum, an herbal formulation comprising gelatin capsules filled with *A. annua* leaf powder has shown moderate activity against *L. panamensis* amastigotes (Mesa et al., 2017). Furthermore, Biliaet al. (2008) has reported that only the organic extracts of *A. annua* arrested the growth of *L. donovani*. These support our results

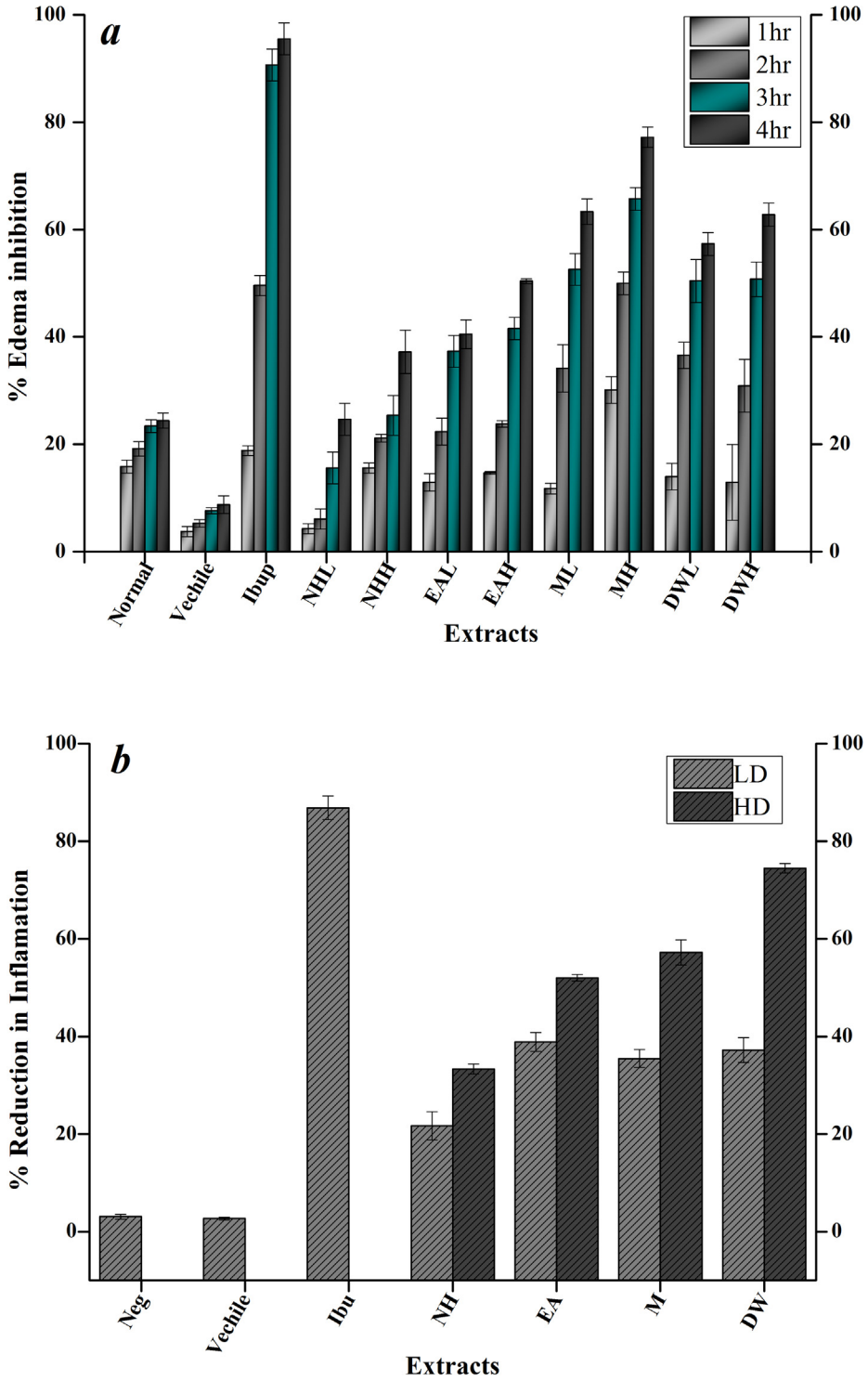

Fig. 6. Percentedema inhibition by *A. brevifolia* extracts. Datavalues(mean ± SD) are average of triplicate analysis. a: Percent of paw edemainhibition, b: Percent of analedemainhibition, Vehicle: 1% Dimethyl sulfoxide, Ibup: Ibuprofen, NHL: Low dose (150 mg/kg) of N-hexane, NHH: High dose (300 mg/kg) of N-hexane, EAL: Low dose (150 mg/kg) of Ethyl acetate, EAH: High dose (300 mg/kg) of Ethyl acetate, ML: Low dose (150 mg/kg) of Methanol, MH: High dose (300 mg/kg) of Methanol, DWL: Low dose (150 mg/kg) of Distilledwater,DWH: High dose (300 mg/kg) of Distilledwaterextracts of *A. brevifolia*.

making us to infer that antileishmanial potential is more prominent in the non-polar extracts of *Artemisia* species.

Continuing the pharmacological profiling of *A. brevifolia*, *in vitro* cytotoxic activity was determined using brine shrimps, isolated lymphocytes and cancer cell lines. Cancer is a global threat that despite extensive research has no complete cure so far (Waseem et al., 2017). About 18 million new cases of cancer were reported in 2018 that are expected toclimbto approximately 29–37 million over the next twenty years. Natural products by virtue of their biochemical specificity and chemical diversity are considered a valuable source for the discovery of novel anticancer leads. Also, according to WHO cancer report 2018, a patient burdened with drug-induced toxicity can get help from the complementary and alternative medicine (Sung et al., 2021).

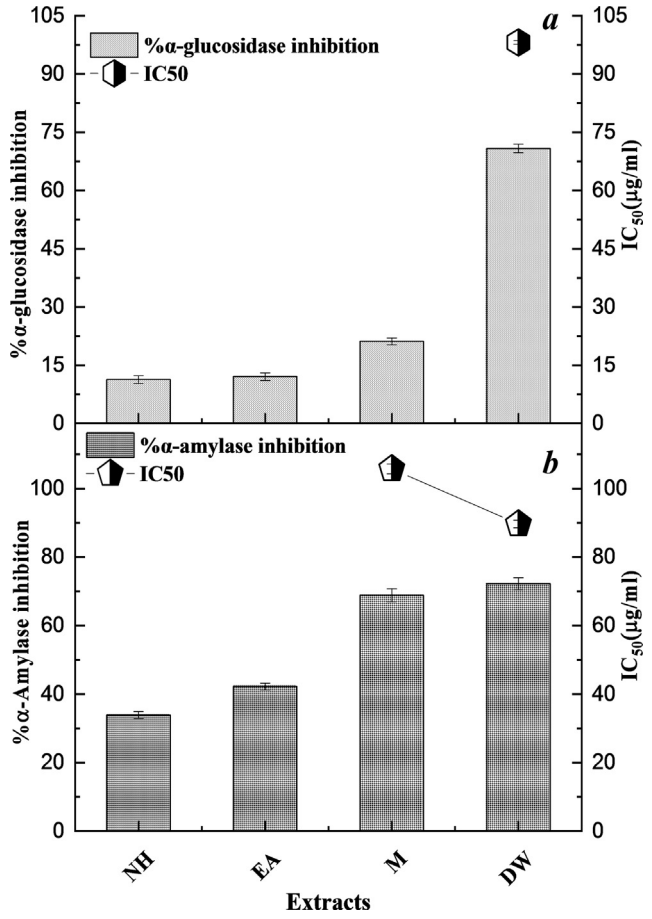

Fig. 7. Enzyme inhibition by *A. brevifolia* extracts.α-glucosidase(a) and α-amylase (b) inhibition potentials are presented as mean ± SD from triplicate investigations. Acarbose exhibited an IC_{50} value of 33.73 ± 0.12 μg/ml.NH: n-Hexane, EA: Ethyl acetate, M: Methanol, DW: Distilled water.

Initially, cytotoxic potential of *A. brevifolia* extracts was assessed against brine shrimps. A positive correlation between the brine shrimp cytotoxicity and human nasopharyngeal carcinoma cell lines (KB cell lines) has been reported thus making the activemoieties prospective targets for antitumor and anticancer activities (Hendra et al., 2021). In the recent study, all the extracts have exhibited a concentration dependent lethality with LD_{50} less than 50 μg/ml. According to the norms of assay, nearly all the extracts possess cytotoxic potential as an LD_{50} less than 1000 μg/ml is considered to be cytotoxic (Fatima et al., 2015). So, the cytotoxic potential of *A. brevifolia* extracts was further gauged against human hepatocarcinoma, leukemia, colon, prostate, breast and ovarian cancer cell lines.

According to WHO cancer report 2018, most frequently diagnosed cancer is female breast cancer (11.6%) followed by colorectal cancers (10.2%). Prostate cancer, hepatoma and leukemia are amongst the most widespread cancers in the world. Cumulatively, these cancers correspond to 54% of all cancer cases and 58% of all deaths (Sung et al., 2021).

Herein, EA was most active against all the cancer cell lines followed by NH and M extracts. According to the RP-HPLC analysis in our study, artemisinin and its derivatives though present in NH and M extract, are more concentrated in EA extract. Artemisinin and its analogs have been reported to exert their antitumor effects by inhibiting cancer proliferation, metastasis, and angiogenesis (Crespo-Ortiz and Wei, 2012). Polyphenolics detected in the extracts, i.e., gallic acid, quinic acid, apigenin, emodin also have well known anticancer profile (Nasir et al., 2020). Therefore, it can be surmised that artemisinin and its derivatives as well as detected antioxidant moieties might be responsible for the significant ($p < 0.05$) anticancer activity of the extracts. Though, plants perceptibly possess therapeutically active moieties; however, safety of the active concentration of these therapeutic moieties must be the prime determinant. This pertinent data can be generated by evaluating toxicity against isolated lymphocytes, which is a suitable alternative of *in vivo* models due to their economic and ethical concerns (Ahmed et al., 2017). Consequently, cytotoxicity of the extracts was assessed against isolated lymphocytes to establish their safety profile. Results clearly indicate the non-toxic behaviour of extracts against the isolated lymphocytes indicating a discerning response that was observed only against cancer cell lines and preventing normal cells to get damaged. On the contrary, vincristine, the positive control used, exhibited significant ($p < 0.05$) cytotoxicity against lymphocytes.

Next, genotoxic evaluation of *A. brevifolia* was conducted using a standard test battery to assess cytogenetic damage. It has been reported that pyrrolizidine alkaloids produced by the plants belonging to Orhidaceae, Boraginaceae, Poaceae and Asteraceae families can damage DNA and other cellular components, which regulate the fidelity of the genome (Schramm et al., 2019). Such genotoxic agents interact with a specific DNA base sequence causing breakage, lesions, deletion, fusion, non-disjunction or segregation leading to damage and mutation. Therefore, testing at earlier stages is imperative for the hazard assessment of natural products to identify genotoxic liabilities. Different endpoints can be anticipated while evaluating genotoxicity, i.e., point mutations induction, changes in chromosome structure (breaks, deletions, rearrangements) or chromosomal number (polyploidy or aneuploidy). No single test can envisage an unequivocal ruling about the genotoxic potential of any substance (Savale, 2018). Thus, comet, micronucleus and chromosomal aberration assays were performed on extracts of *A. brevifolia*.

Comet assay, being highly sensitive, detects single and double strand breaks, repair induced breaks, alkali labile lesions and abasic sites even at a single cell level and is called single-cell gel electrophoresis (Majid et al., 2018). Breakage of supercoiled DNA leaves it un-winded, which then extends out of the gel layer and appears as a comet under electrophoresis at high pH. Relative intensity of comets' tail DNA is directly proportional to DNA breakage frequency (Kazmi et al., 2018).

Currently, maximum DNA ($p < 0.05$) damage was produced by 5-Fluorouracil, which is evident from the migration of 32.15% of DNA to comet's tail. On the contrary, the extracts showed minimal formation of comets' tail. Furthermore, cytogentic damage was evaluated using micronucleus and chromosomal aberration assay. Micronucleus assay involves the identification of a small, membrane bounded DNA fragment in the cytoplasm of the cell called micronuclei, which may originate from acentric chromosome fragments or whole chromosomes. The increased micronuclei formation indicates the frequency and severity of DNA damage. Assay comprehensively investigate both aneugens and clastogens as well as other cellular and nuclear dysfunctions (Tsuboy et al., 2007). It also measures the NDI, which itself is a measure of genomic aberration. The rationale behind NDI measurement is that the cells with greater chromosomal damage are less likely to enter cell division or cell death occurs before cell division. If the cells fail to divide during the cytokinesis-block phase, they will remain mono-nucleated with the lowest NDI value of 1.0. If binucleated cells are formed after completing one division, NDI will be 2.0 and so on (İpek et al., 2017).

In current study, no significant percent of micronucleus formation was observed in extract groups and the NDI was signif-

icantly ($p < 0.05$) higher than positive control cisplatin. Subsequent analysis of chromosomal aberration showed that the extracts did not induce DNA damage. The cell lines were treated with a direct mutagen, cisplatin, which is known to cause inter and intrastrand DNA crosslinks. It perturbs DNA replication and transcription eventually leading to cell cycle arrest and cell apoptosis. Drug develops structural aberrations by inducing chromatid or chromosomal breaks (Imreova et al., 2017). Here, an anticlastogenic activity was revealed against cisplatin in extract treated groups. It can be explained by the increased detoxification or excessive DNA repair stimulation by virtue of strong antioxidant assertiveness of the extracts (Kazmi et al., 2018). These results showed that the extracts of *A. brevifolia* are not genotoxic, supporting their use by the natives of Northern areas of Pakistan. It can also be inferred that the extracts have exerted their significant ($p < 0.05$) cytotoxic potential through a mechanism other than DNA damage, which needs to be investigated through further studies.

Natural products with antioxidant and cytotoxic potentials are expected to have anti-inflammatory profile as well. This is based on the fact that reactive oxygen species are the prime mediators for oxidative stress and inflammation. Nitric oxide, an important chemical mediator of oxidation and inflammation, is involved in the regulation of numerous physiological processes but its excessive production brings about deleterious effects (Farooq et al., 2020). It reacts with oxygen under aerobic conditions and generates highly reactive intermediate species, i.e., nitrate, nitrite and peroxynitrite, which can induce oxidative stress. Therefore, inhibition of NO production serves as a key factor for the screening of drugs with anti-inflammatory potential (Fatima et al., 2020). Moreover, many debilitating diseases including rheumatoid arthritis, diabetes, cancer and depression root back to inflammatory processes. Despite the availability of various anti-inflammatory drugs in the market, there is an overall shift from synthetic drugs to natural therapy (Karimi et al., 2015). In line with this, we evaluated the *in vitro* and *in vivo* anti-inflammatory activity of *A. brevifolia* extracts. M and DW extracts showed highest inhibition of NO. Furthermore, results of *in vivo* paw andanal edema models also presented M and DW extracts as potent anti-inflammatory agents as compared to other extracts. Maximum phenolic and flavonoid contents were preliminarily quantified in these extracts, which can be related to their anti-inflammatory potential. Being rich in bioactive polyphenolics, these extracts quenched NO thus halting the production of highly reactive intermediates by consuming available oxygen. Similarly, M and DW extracts were found to be rich in caffeoylquinic acids, apigenin, gallic acid and jasmonic acid. All of these compounds have established anti-inflammatory profile (Gutiérrez-Grijalva et al., 2018).

Lastly, the pharmacological evaluation of *A. brevifolia* extracts was extended to determine the inhibition of carbohydrate-metabolizing enzymes by the extracts. Inhibitors of carbohydrate- metabolizing enzymes α-amylase and α-glucosidase have offered new avenues for the management of postprandial blood glucose level. Found in saliva and pancreatic juice, α-amylases hydrolyzes the large insoluble starch molecules to soluble oligosaccharides, which are converted to glucose molecules by the α-glucosidases present in the brush-border surface membrane of small intestine (Ahmed et al., 2019). This leads to a rise in blood glucose levels, which can be debilitating for patients of diabetes mellitus. Inhibition of α-amylase and α-glucosidase enzymes can reduce the cleavage of complex carbohydrates into glucose that will aid in the management of postprandial hyperglycemia in diabetes patients. Chronic hyperglycemia augments the generation of ROS, accentuating the oxidative damage, which ultimately curtails the insulin secretion with concurrent negative regulation of insulin signaling cascade (Ahmed et al., 2017).

In the present work, DW and M extracts demonstrated a significant ($p < 0.05$) inhibition of α-amylase and α-glucosidase enzymes. The α-amylase inhibition potential of DW extract is somewhat analogues to that of standard acarbose. Numerous plant-derived secondary metabolites including phenolic compounds, and flavonoids have been proven to possess α-amylase and α-glucosidase inhibitory activities. In the current study, a substantial amount of phenolics and flavonoids including apigenin, jasmonic acid and caffeoylquinic acid has been detected in DW extract. Apigenin has been reported for its α- amylase activity (Wang et al., 2010). Previously, mono, di and tri-substituted caffeoylquinic acid were found to be the predominant phenolic group of Siberian *Artemisia* species, responsible for α-amylase and α-glucosidase inhibitory activities (Olennikov et al., 2018). Moreover, studies have reported that jasmonic acid elicitation has improved the anti-α-amylase potential of several essential oils (Złotek et al., 2020). Mass spectroscopy of DW extract has revealed the presence of these compounds. Therefore, substantial carbohydrate-metabolizing inhibition by distilled water extract might be accredited to the presence of these compounds.

5. Conclusions

In conclusion, the current study presents *A. brevifolia*as a rich source of artemisinin and its derivatives, which might have played the key role in several of its pharmacological attributes, i.e., antimalarial, anticancer and antidiabetic activities. The EA extract showed good antimalarial and antileishmanial activities especially against resistant malarial strain. Manifestation of important secondary metabolites including phenolics and flavonoids supports substantial antioxidant properties of the extracts. Significant anti-inflammatory potential deemed these extracts as suitable candidates for detailed evaluation at molecular level. Noteworthy anti-bacterial potential especially against resistant strains justifies its ethnopharmacological use to treat a number of infections. Moreover, the results of genotoxic assays confirm the safe behavior of the plant and also helped to infer that the extracts have exerted their significant cytotoxic potential through a mechanism other than DNA damage, which needs to be investigated through further studies.

Declaration of Competing Interest

The authors declare that they have no known competing financial interests or personal relationships that could have appeared to influence the work reported in this paper.

Acknowledgements

The authors would like to acknowledge the Deanship of scientific research, Qassim University for funding the publication of this project. Authors would also like to acknowledge Prof. Dr. RizwanaAleem Qureshi, Department of Plant sciences, Faculty of Biological sciences, Quaid-i-Azam University, Islamabad, Pakistan for identifying the plant sample. Moreover, authors are thankful to Dr. Durdana Waseem for proof-reading the manuscript.

Funding

The research work of current project was funded by Higher Education commission, Pakistan through National Research Program for Universities (HEC/NRPU-QAU-7528).

Availability of data

We hereby confirm that all the data produced in the manuscript is original based on extensive repeated experimentation and can be provided upon reasonable request, when needed.

Ethics approval and consent to participate

International ethical guidelines were followed for lymphocytes isolation, after approval by the Ethical Board of the Quaid-i-Azam University, Islamabad, Pakistan (Letter # BEC-FBS-QAU -042/2019). We further confirm that any aspect of the work covered in this manuscript that involved experimental animals has been conducted after approval of experimental protocol (Letter # BEC-FBS-QAU -067/2019) and animal usage (Letter # BEC-FBS-QAU -089/2019) from the Institutional Animal Ethics Committee.

Contributions

We hereby confirm that all authors have made considerable contribution to the work and approved the final version of publication. IH conceptualized and designed the study, supervised execution of experiments, critically revised the manuscript and approved the final version of this manuscript. STBK performed experiments, analyzed and interpreted the data, wrote and revised the manuscript. IN contributed in data curation, validation and critical revision of the final version of the manuscript. HN contributed in the conduction of experiments and acquisition of the data. HF contributed in study design and data validation. ASF contributed in data validation and critical revision of the revised version of the manuscript.

References

Abu-Lafi, S., Akkawi, M., Al-Rimawi, F., et al., 2020. Morin, quercetin, catechin and quercitrin as novel natural antimalarial candidates.

Ahmed, M., M. Adil, I.-u.-. Haq, et al., 2019. RP-HPLC-based phytochemical analysis and diverse pharmacological evaluation of Quercusfloribunda Lindl. ex A. Camus nuts extracts. Natl. Prod. Res. 1–6.

Ahmed, M., Fatima, H., Qasim, M., et al., 2017. Polarity directed optimization of phytochemical and in vitro biological potential of an indigenous folklore: Quercusdilatata Lindl. ex Royle. BMC Complement Altern. Med. 17, 1–16.

Akrout, A., Gonzalez, L.A., El Jani, H., et al., 2011. Antioxidant and antitumor activities of Artemisiacampestris and Thymelaeahirsuta from southern Tunisia. Food Chem. Toxicol. 49, 342–347.

Ashraf, M., Hayat, M.Q., Jabeen, S., et al., 2010. Artemisia L. species recognized by the local community of the northern areas of Pakistan as folk therapeutic plants. J. Med.Plants Res.

Baek, J., Lee, T.K., Song, J.-H., et al., 2018. Lignan glycosides and flavonoid glycosides from the aerial portion of Lespedezacuneata and their biological evaluations. Molecules 23, 1920.

Baig, M.W., Nasir, B., Waseem, D., et al., 2020. Withametelin: a biologically active withanolide in cancer, inflammation, pain and depression. SPJ 28, 1526–1537.

Bilia, A.R., Kaiser, M., Vincieri, F.F. et al., 2008. Antitrypanosomal and antileishmanial activities of organic and aqueous extracts of Artemisiaannua. Nat. Prod. Commun. 3, 1934578X0800301204.

Crespo-Ortiz, M.P., Wei, M.Q. 2012. Antitumor activity of artemisinin and its derivatives: from a well-known antimalarial agent to a potential anticancer drug. J Biomed Biotechnol. 2012,

De Sarkar, S., Sarkar, D., Sarkar, A., et al., 2019. The leishmanicidal activity of artemisinin is mediated by cleavage of the endoperoxide bridge and mitochondrial dysfunction. Parasitology 146, 511–520.

EREL, Ş. B., G. Reznicek, S. G. Şenol, et al., 2012. Antimicrobial and antioxidant properties of Artemisia L. species from western Anatolia. Turkish J. Biol. 36, 75–84.

Farooq, S., Mazhar, A., Ghouri, A., et al., 2020. One-Pot Multicomponent Synthesis and Bioevaluation of Tetrahydroquinoline Derivatives as Potential Antioxidants, α-Amylase Enzyme Inhibitors. Anti-Cancerous and Anti-Inflammatory Agents. Molecules. 25, 2710.

Fatima, H., Ahmed, M., Baig, M.W., et al., 2020. Cancer Chemopreventive and Cytotoxic Activities of Isowithametelin from Datura innoxia. Rev. Bras. Farmacogn. 30, 723–728.

Fatima, H., Khan, K., Zia, M., et al., 2015. Extraction optimization of medicinally important metabolites from Datura innoxia Mill.: an in vitro biological and phytochemical investigation. BMC Complement Altern. Med. 15, 1–18.

Gutiérrez-Grijalva, E.P., Picos-Salas, M.A., Leyva-López, N., et al., 2018. Flavonoids and phenolic acids from oregano: Occurrence, biological activity and health benefits. Plants 7, 2.

Hayat, M.Q., Khan, M.A., Ashraf, M. et al., 2009. Ethnobotany of the genus *Artemisia* L.(Asteraceae) in Pakistan.

Hendra, R., Khodijah, R., Putri, R., et al., 2021. Cytotoxicity and Antiplasmodial Properties of Different Hylocereuspolyrhizus Peel Extracts. Med. Sci. Monit. Basic Res. 27, e931118–e1931111.

Imreova, P., Feruszova, J., Kyzek, S., et al., 2017. Hyperforin exhibits antigenotoxic activity on human and bacterial cells. Molecules 22, 167.

İpek, E., Ermiş, E., Uysal, H., et al., 2017. The relationship of micronucleus frequency and nuclear division index with coronary artery disease SYNTAX and Gensini scores. Anatolian J. Cardiol. 17, 483.

Iqbal, S., Younas, U., Chan, K.W., et al., 2012. Chemical composition of Artemisiaannua L. leaves and antioxidant potential of extracts as a function of extraction solvents. Molecules 17, 6020–6032.

Kaou, A.M., Mahiou-Leddet, V., Hutter, S., et al., 2008. Antimalarial activity of crude extracts from nine African medicinal plants. J. Ethnopharmacol. 116, 74–83.

Karimi, A., Majlesi, M., Rafieian-Kopaei, M., 2015. Herbal versus synthetic drugs; beliefs and facts. J. Nephropharmacol. 4, 27.

Kazmi, S.T.B., Majid, M., Maryam, S., et al., 2018. Quercusdilatata Lindl. ex Royle ameliorates BPA induced hepatotoxicity in Sprague Dawley rats. Biomed. Pharmacother. 102, 728–738.

Koul, B., Taak, P., Kumar, A., et al., 2018. The Artemisia genus: A review on traditional uses, phytochemical constituents, pharmacological properties and germplasm conservation. JGL 7, 1–7.

Lin, S., McCauley, E.P., Lorig-Roach, N., et al., 2017. Another Look at Pyrroloiminoquinone Alkaloids—Perspectives on Their Therapeutic Potential from Known Structures and Semisynthetic Analogues. Mar. Drugs. 15, 98.

Liu, Y., lü, H., Pang, F. 2009. Solubility of artemisinin in seven different pure solvents from (283.15 to 323.15) K. J. Chem. Eng. 54, 762–764.

Majid, M., Khan, M.R., Shah, N.A., et al., 2015. Studies on phytochemical, antioxidant, anti-inflammatory and analgesic activities of Euphorbiadracunculoides. BMC Complement Altern. Med. 15, 1–15.

Majid, M., Nasir, B., Zahra, S.S., et al., 2018. Ipomoeabatatas L. Lam. ameliorates acute and chronic inflammations by suppressing inflammatory mediators, a comprehensive exploration using in vitro and in vivo models. BMC Complement Altern. Med. 18, 1–20.

Mesa, L.E., Vasquez, D., Lutgen, P., et al., 2017. Invitro and invivo antileishmanial activity of Artemisiaannua L. leaf powder and its potential usefulness in the treatment of uncomplicated cutaneous leishmaniasis in humans. Rev. Soc. Bras. Med. Trop. 50, 52–60.

Mourad, B., Rachid, B., Sihem, B., 2018. Antioxidant activity and phenolic content of Artemisiacampestris from two regions of Algeria. World J. Environ. Biosci. 7, 61–66.

Nadeem, M., Shinwari, Z.K., Qaiser, M., 2013. Screening of folk remedies by genus Artemisia based on ethnomedicinal surveys and traditional knowledge of native communities of Pakistan. Pak. J. Bot. 45, 111–117.

Nasir, B., Ahmad, M., Zahra, S.S., et al., 2017. Pharmacological evaluation of Fumariaindica (hausskn.) Pugsley; a traditionally important medicinal plant. Pak. J. Bot. 49, 119–132.

Nasir, B., Baig, M.W., Majid, M., et al., 2020. Preclinical anticancer studies on the ethyl acetate leaf extracts of Daturastramonium and Daturainoxia. BMC Complement Med. Therap. 20, 1–23.

O'neill, P.M., Barton, V.E., Ward, S.A. 2010. The molecular mechanism of action of artemisinin—the debate continues. Molecules. 15, 1705–1721.

Olennikov, D.N., Chirikova, N.K., Kashchenko, N.I., et al., 2018. Bioactive phenolics of the genus Artemisia (Asteraceae): HPLC-DAD-ESI-TQ-MS/MS profile of the Siberian species and their inhibitory potential against α-amylase and α-glucosidase. Front. Pharmacol. 9, 756.

Organization, W.H., 2016. World malaria report 2015. World Health. Organization.

Ovais, M., Ayaz, M., Khalil, A.T., et al., 2018. HPLC-DAD finger printing, antioxidant, cholinesterase, and α-glucosidase inhibitory potentials of a novel plant Olaxnana. BMC Complement Altern. Med. 18, 1–13.

Parameswari, P., Devika, R., Vijayaraghavan, P., 2019. Invitro anti-inflammatory and antimicrobial potential of leaf extract from Artemisianilagirica (Clarke) Pamp. Saudi J of Biol. Sci. 26, 460–463.

Rohmer, M., 1999. Isoprenoids including carotenoids and steroids. Compreh. Natl. Prod. Chem. 2, 45.

Savale, S.K., 2018. Genotoxicity of Drugs: Introduction, Prediction and Evaluation. AJBR 4, 1–29.

Schramm, S., Köhler, N., Rozhon, W., 2019. Pyrrolizidine alkaloids: biosynthesis, biological activities and occurrence in crop plants. Molecules 24, 498.

Seenivasagan, T., Sharma, K.R., Sekhar, K., et al., 2009. Electroantennogram, flight orientation, and oviposition responses of Aedes aegypti to the oviposition pheromone n-heneicosane. Parasitol. Res. 104, 827–833.

Shelar, D., Shirote, P., 2011. Natural product in drug discovery: back to future. Biomed. Pharmacol. J. 4, 141.

Sibmooh, N., Udomsangpetch, R., Kijjoa, A., et al., 2001. Redox reaction of artemisinin with ferrous and ferric ions in aqueous buffer. Chem. Pharm. Bull. 49, 1541–1546.

Srinivasulu, C., Ramgopal, M., Ramanjaneyulu, G., et al., 2018. Syringic acid (SA)-a review of its occurrence, biosynthesis, pharmacological and industrial importance. Biomed. Pharmacother. 108, 547–557.
Sung, H., Ferlay, J., Siegel, R.L., et al., 2021. Global cancer statistics 2020: GLOBOCAN estimates of incidence and mortality worldwide for 36 cancers in 185 countries. CA: Cancer. J. Clin. 71, 209–249.
Tsuboy, M., Angeli, J., Mantovani, M., et al., 2007. Genotoxic, mutagenic and cytotoxic effects of the commercial dye CI Disperse Blue 291 in the human hepatic cell line HepG2. Toxicol. InVitro. 21, 1650–1655.
Wang, H., Du, Y.-J., Song, H.-C., 2010. α-Glucosidase and α-amylase inhibitory activities of guava leaves. Food Chem. 123, 6–13.
Waseem, D., Butt, A.F., Haq, I.-U., et al., 2017. Carboxylate derivatives of tributyltin (IV) complexes as anticancer and antileishmanial agents. DARU J. Pharm. Sci. 25, 1–14.
Zahra, S.S., Ahmed, M., Qasim, M., et al., 2017. Polarity based characterization of biologically active extracts of Ajugabracteosa Wall. ex Benth. and RP-HPLC analysis. BMC Complement Altern. Med. 17, 1–16.
Złotek, U., Rybczyńska-Tkaczyk, K., Michalak-Majewska, M., et al., 2020. Potential Acetylcholinesterase, Lipase, α-Glucosidase, and α-Amylase Inhibitory Activity, as well as Antimicrobial Activities, of Essential Oil from Lettuce Leaf Basil (Ocimum basilicum L.) Elicited with Jasmonic Acid. App Sci. 10, 4315.